

Article

Marine Biodiversity in Inútil Bay (Tierra del Fuego): Patterns of Zooplanktonic and Benthic Assemblages

Benjamín Rodríguez-Stepke ^{1,2,*}, Américo Montiel ³, Jonathan Poblete ¹, Mauricio F. Landaeta ^{2,4}, Daniel Pérez ³, Jorge Pérez-Schultheiss ⁵, Kharla Skamiotis ², Ignacio Garrido ⁶, Fernanda S. Orrego ² and Mathias Hüne ¹

¹ Fundación Rewilding Chile, Puerto Varas 5550000, Chile; jonathan.poblete@rewildingchile.org (J.P.); mathias.hune@rewildingchile.org (M.H.)

² Laboratorio de Ictiología e Interacciones Biofísicas (LABITI), Instituto de Biología, Facultad de Ciencias, Universidad de Valparaíso, Valparaíso 2362700, Chile; landaeta.mauricio@gmail.com (M.F.L.); fernanda.orrego.a@gmail.com (F.S.O.)

³ Laboratorio de Ecología Funcional, Instituto de la Patagonia, Universidad de Magallanes, Punta Arenas 6210427, Chile; americo.montiel@umag.cl (A.M.)

⁴ Centro de Observación y Análisis del Océano Costero (COSTA-R), Universidad de Valparaíso, Valparaíso 2362700, Chile

⁵ Área Zoología de Invertebrados, Museo Nacional de Historia Natural de Chile, Casilla 787, Santiago 8320096, Chile

⁶ Laboratorio Costero de Recursos Acuáticos de Calfuco (ICML), Facultad de Ciencias, Universidad Austral de Chile, Valdivia 5110566, Chile

* Correspondence: benja.rodriguez.stepke@gmail.com

Abstract

Southern Patagonian ecosystems are characterized by high environmental heterogeneity. Within this context, Inútil Bay exhibits a complex geomorphology and only fragmentary information on its biodiversity, despite a long history of resource exploitation and increasing human pressures. The objective of this study was to establish a baseline of biodiversity focusing on three key trophic components: zooplankton, megabenthos, and macrobenthos. Samples were collected using both traditional and non-invasive methods, including a bongo net, ROV, and Van Veen grab. A total of 239 taxa were identified, comprising 32 zooplankton species, 61 megabenthic taxa, and 146 macrobenthic taxa. Alpha diversity indices revealed a spatial gradient, with higher mixed-level taxonomic richness near the Whiteside Channel. In contrast to patterns observed in zooplankton and megabenthos, the macrofauna showed significant differences between assemblages at stations located inside and outside the bay. Moreover, a low representation of meroplankton was recorded compared to the high abundance of adult benthic invertebrates. Overall, these results provide a biodiversity baseline, underscore the ecological vulnerability of Inútil Bay, and support its recognition as a priority area for conservation.

Keywords: community structure; Magellan province; benthic macrofauna; zooplankton



Academic Editor: Bert W. Hoeksema

Received: 22 September 2025

Revised: 15 October 2025

Accepted: 16 October 2025

Published: 1 November 2025

Citation: Rodríguez-Stepke, B.; Montiel, A.; Poblete, J.; F. Landaeta, M.; Pérez, D.; Pérez-Schultheiss, J.; Skamiotis, K.; Garrido, I.; Orrego, F.S.; Hüne, M. Marine Biodiversity in Inútil Bay (Tierra del Fuego): Patterns of Zooplanktonic and Benthic Assemblages. *Diversity* **2025**, *17*, 763. <https://doi.org/10.3390/d17110763>

Copyright: © 2025 by the authors. Licensee MDPI, Basel, Switzerland. This article is an open access article distributed under the terms and conditions of the Creative Commons Attribution (CC BY) license (<https://creativecommons.org/licenses/by/4.0/>).

1. Introduction

Over the past century, the study of biodiversity has faced major challenges in both scientific and political spheres. Although significant progress has been made internationally, biodiversity remains a subject of intense debate with persistent knowledge gaps [1]. This situation is particularly critical in the sub-Antarctic regions at the southern tip of South America, where the available information on biodiversity is fragmentary, spatially restricted,

and temporally discontinuous [2]. In this context, documenting marine biodiversity in areas under increasing pressure, mainly due to human presence, has become a priority, given the expansion of aquaculture concessions [3,4], the development of large-scale green hydrogen projects [5,6], and fisheries [7], the latter being one of the main economic drivers in the Magallanes region, where Inútil Bay is located.

Biodiversity studies in Inútil Bay are scarce, sporadic, and largely site-specific. For instance, much of the current knowledge of zooplankton originates from the CIMAR program (Marine Research Cruises in Remote Areas, in Spanish), which has been limited to a single station within the bay. These efforts quantified zooplankton biomass and ichthyoplankton [8,9], reporting low abundances ($<65 \text{ ind} \cdot 1000 \text{ m}^{-3}$) and a limited presence of fish larvae. Additional work has addressed trophic interactions of early fish stages at the bay's mouth and adjacent sectors [10]. While studies exist on specific zooplankton groups in Inútil Bay [8–13], no integrated assessment of zooplankton and ichthyoplankton biodiversity with broad spatial coverage is yet available. Such knowledge is essential to identify species, understand the factors controlling their dynamics, evaluate their role in the food web, particularly as prey for seabirds and marine mammals and inform management actions. This need is underscored by the bay's long history of marine resource exploitation, which has included species of commercial interest with meroplanktonic phases such as the razor clam (*Ensis macha*), octopus (*Enteroctopus megalocyathus*), whelk (*Trophon geversianus*), and king crab (*Lithodes santolla*).

Research on benthic fauna, by contrast, has focused primarily on the abundance and richness of macrofauna, especially polychaetes [14–16], but also echinoderms [17–19], mollusks [15,18], and amphipods [16]. Recent studies have demonstrated ecological connectivity between Inútil Bay and Almirantazgo Sound, with Polychaeta, Mollusca, and Arthropoda as the most representative groups [16]. In recent years, however, the use of underwater imagery (photographs and video) has gained increasing prominence as a scientific tool for ecological assessment, owing to its non-destructive nature [20], reduced costs, and technological improvements [21]. Within southern Chile, important advances have been achieved through photographic surveys across fjords, the Beagle Channel, and the Strait of Magellan [22–24]. In northern Patagonia, studies in the Comau Fjord [25] and Puyuhuapi Fjord [26,27] have reported diverse benthic assemblages, while more recent efforts in the Katalalixar National Reserve have provided valuable new data [28]. Yet, to date, no study has applied such approaches in the extensive territory of Inútil Bay. This study therefore seeks to provide novel insights into the composition of its megabenthic communities.

Comparative analyses of sub-Antarctic marine communities involving more than two ecological groups sampled simultaneously remain rare. Most studies have focused on a single fraction of the ecosystem, offering a limited perspective that overlooks the interconnected nature of these complex systems. In this context, conducting an integrated study across a broad spectrum of biodiversity was made possible through the collaboration of experts in multiple marine taxa. Here, we present the results of expeditions conducted in 2024 in Inútil Bay, combining zooplankton surveys, non-invasive underwater video systems for megabenthic observations, and Van Veen grab sampling for benthic macrofauna. Our primary objective was to establish a baseline of marine biodiversity in the area, providing critical data to support a potential marine protected area proposal and to contribute to the conservation of this unique ecosystem within the Magallanes marine ecoregion [29,30].

2. Materials and Methods

2.1. Study Area

Inútil Bay ($53^{\circ}30' \text{ S}$, $69^{\circ}30' \text{ W}$) is located on the northwestern coast of Tierra del Fuego Island, southern Chile. The bay originated during the Late Pleistocene, when deglaciation

events about 14,000 years ago led to the retreat of the Darwin Range ice towards the east, forming a broad and topographically uniform basin. Inútil Bay is part of the Magdalena Sound–Puerto del Hambre–Paso Ancho sub-basin, where the combined action of strong tidal currents, persistent winds, and seafloor topography promotes a well-mixed water column that counteracts stratification caused by freshwater inputs [31]. As a result, local water masses are mainly defined by thermohaline properties modulated by continental runoff, tidal regime, and wind patterns.

The bay is semi-enclosed and southwestward oriented, extending approximately 100 km in length and 50 km in average width, with a total surface area of about 4776 km². Its mouth lies at Cape Boquerón, where maximum depths reach nearly 250 m near the Whiteside Channel. The rest of the bay shows a relatively uniform bathymetry, with depths generally around 25 m that gradually increase toward the mouth [15]. Inútil Bay connects directly to the Strait of Magellan through Cape Boquerón and to Almirantazgo Sound via the Whiteside Channel, which separates it from Dawson Island (Figure 1).

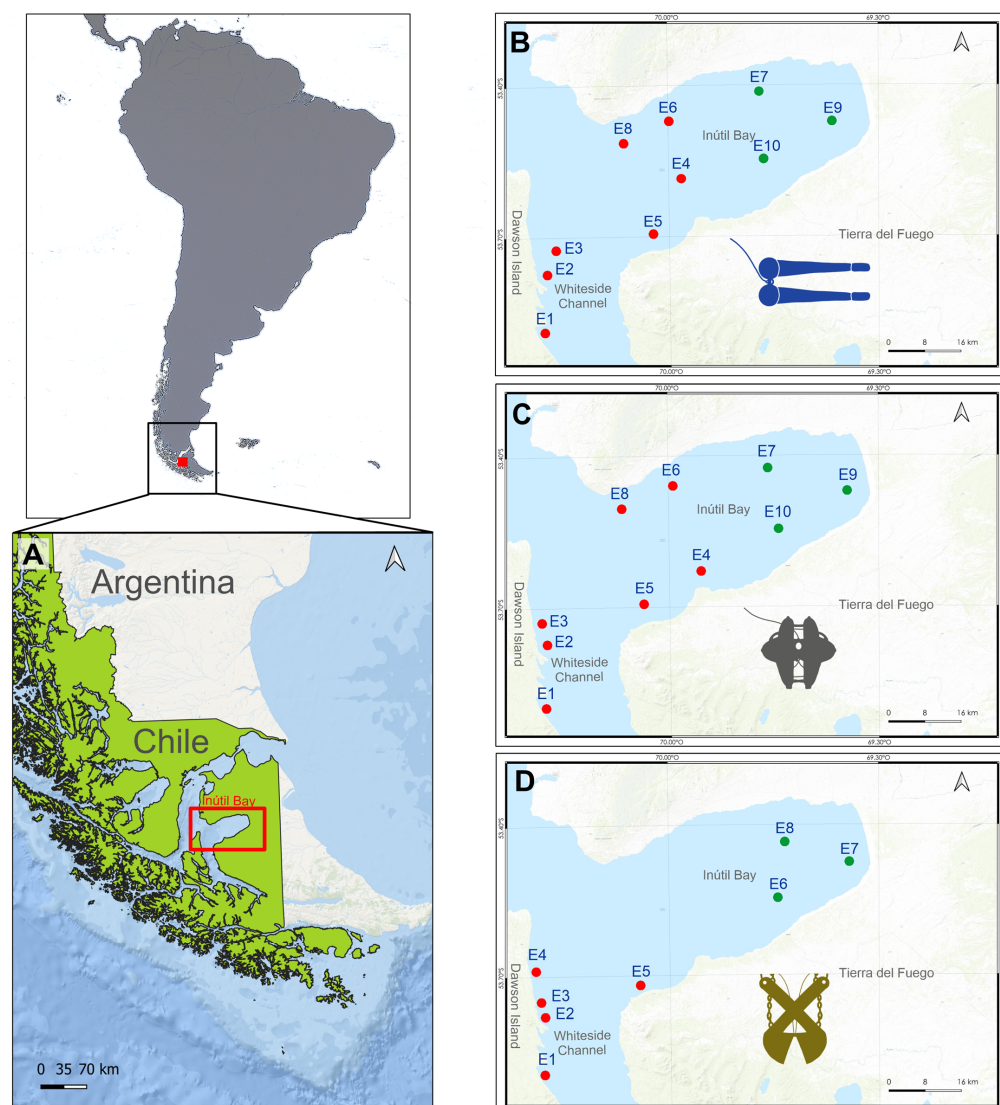


Figure 1. Study area maps. **Left panel:** (A). Geographical location of Inútil Bay in southern Chilean Patagonia. **Right panel:** detailed view of the study area showing the numbered sampling stations; green dots indicate stations inside the bay, while red dots represent external and adjacent sites. Each symbol denotes the methodology applied to study community assemblages: (B). Zooplankton (Bongo net sampling), (C). Megabenthic fauna (ROV DTG3), (D). Soft-bottom macrofauna (Van Veen grab).

The system receives substantial freshwater inputs from at least ten rivers, most of them located on the eastern side of the fjord, including the Rosario, Esperanza, and Discordia (northern shore); Marazzi and Centenario (southeastern shore); and Torcido, Macklelland, Ana, Blanco, and Woodsend (southern shore).

Sediment composition varies across the bay. Sandy sediments dominate the northern and eastern shores, whereas mixed sediments, sand with mud and muddy sand, are more common along the southern coast. More broadly, the seafloor consists mainly of mud interspersed with sand and gravel, reflecting high structural heterogeneity [32]. Oceanographically, the northern sector of Inútil Bay exhibits surface temperatures exceeding 6.5 °C. Mean surface salinity is 30.46 g kg⁻¹, with values above 31.0 g kg⁻¹ recorded at the head of the bay. At depths greater than 100 m, salinity ranges between 31.0 and 32.0 g kg⁻¹ [33].

Fieldwork was carried out from 10 to 14 July 2024, covering Inútil Bay and adjacent areas (Figure 1). Sampling included: (i) zooplankton collection (Figure 1A); (ii) visual surveys of megabenthic assemblages using remotely operated vehicle (ROV) transects (Figure 1B); and (iii) sampling of soft-bottom-associated macrofauna (Figure 1C).

2.2. Zooplankton Sampling

Zooplankton sampling was conducted along transects at stations located both inside and outside Inútil Bay (Figure 1B). At each station, oblique tows were performed from 100 m depth to the surface, or to 10 m above the seafloor in shallow areas (Table A1), using a 60 cm diameter Bongo net fitted with a 300 µm mesh and a TSK flowmeter to estimate filtered water volume. Tows lasted 20–35 min depending on site depth. To ethically euthanize any fish larvae that might have been present in the samples, benzocaine (BZ-20®, Veterquímica, Región Metropolitana, Chile) was added to the sample prior to fixation in 5% buffered formalin with sodium borate. After 24 h, the samples were transferred to 70% ethanol for laboratory analysis. Each sample was thoroughly examined under a Leica EZ4 stereomicroscope (Leica Microsystems, Wetzlar, Germany). Zooplankton organisms were counted and identified to the lowest possible taxonomic level using specialized literature [34–36] and categorized as either holoplankton or meroplankton [37].

2.3. Megabenthic Sampling

Megabenthic invertebrates (>10.0 mm) [38] were surveyed through transects conducted with remotely operated vehicles (ROVs) at depths ranging from 25 to 150 m (Figure 1C; Table A1). Two ROV models were used: DTG3 (Deep Trekker, Kitchener, ON, Canada) and BlueROV2 (Blue Robotics, Torrance, CA, USA), deployed from separate vessels, each equipped with an echosounder, a portable unit on the auxiliary vessel and a fixed unit on the main vessel. Echosounders were used to determine depth and locate areas with homogeneous substrates. Each transect lasted 10 min at a constant speed of 10 m·min⁻¹, covering approximately 100 m in length, with the ROVs maintained 1 m above the seafloor to ensure focus and stability of the video recordings.

Video footage was processed using the online platform BIIGLE (Bio-Image Indexing and Graphical Labelling Environment) [39]. After uploading the recordings to the “Storage” module (which required approximately 24 h for validation), a main project was created, assigning separate “Volumes” to each locality. Taxonomic identification was performed by configuring a list of “Labels” with standardized nomenclature for each species or group of interest. Videos were systematically reviewed, and every organism observed along the transects was annotated using the platform’s labeling tools and the predefined “Labels” list.

2.4. Macrobenthic Sampling

Sediment samples were collected using a 0.15 m² Van Veen grab. A total of 22 samples were obtained at eight stations, at depths ranging from 28 to 50 m (Figure 1D; Table A1).

Each station was sampled once with two replicates, except for station 5, where only one sample could be collected.

For the analysis of benthic macrofauna (>1.0 mm [or >0.5 mm]) [39], samples were sieved on site through a 0.5 mm mesh and preserved in 10% buffered formalin (with borax).

In the laboratory, samples were re-sieved through a 0.5 mm mesh and examined in fractions under an Olympus SZ61 stereomicroscope (Olympus, Tokyo, Japan). Organisms were identified to the lowest possible taxonomic level using specialized literature [40–46].

All individuals were counted, except those with clonal growth (e.g., sponges and ascidians), which were recorded as presence/absence only and excluded from the statistical analysis.

2.5. Statistical Analyses

Alpha diversity was quantified as mixed-level taxonomic richness, Simpson's diversity (1—D; hereafter D'), and Pielou's evenness (J'). D' considers both mixed-level taxonomic richness and relative abundance, while J' measures the evenness of individuals among taxa (range: 0 = maximum inequality; 1 = maximum evenness). Calculations were performed in PAST v4.03 [47]. Because taxa were identified at mixed hierarchical levels (from phylum to species), richness was interpreted as mixed-level taxonomic richness following [48], rather than strict species richness.

Zooplankton abundances were standardized to individuals per 1000 m³ (ind. 1000 m⁻³) and log-transformed ($\log_{10}(x + 1)$) for multivariate analyses, while spatial distributions were expressed as individuals per m² (ind. m⁻²). For megabenthic communities, absolute abundance (MaxN), defined as the maximum number of individuals observed per station in ROV transects, was used. In the case of soft-bottom macrofauna, abundances were standardized to individuals per square meter (ind. m⁻²) and fourth-root transformed ($x^{0.25}$).

Based on abundance data of zooplankton and benthic communities, a one-way PERMANOVA using the Bray–Curtis similarity matrix was applied to assess differences in community composition. In addition, non-metric multidimensional scaling (nMDS) using the same Bray–Curtis similarity matrix on abundance data was performed to visualize spatial patterns in zooplankton, megabenthic, and macrobenthic communities. Furthermore, percentage similarity analysis (SIMPER) was applied to decompose variability in community composition and identify the species contributing most to significant differences among groups. All multivariate analyses were conducted in PRIMER-e v7 [49].

3. Results

3.1. Zooplankton Assemblages

A total of 32 taxa were identified from 7 phyla, of which 25 corresponded to holoplankton and 7 to meroplankton (Table A2). Within the holoplankton, the most abundant taxa were crustaceans of the order Ostracoda, representing 51% of the total abundance (median, 25–75% quartiles; 0.055, 0.012–6.653 ind. m⁻³), the copepod *Clausocalanus brevipes* with 20.8% dominance (0.22, 0.078–0.827 ind. m⁻³), and *Clausocalanus arcuicornis* with 6.2% dominance (0.017, 0.009–0.351 ind. m⁻³). The high abundance of ostracods was due to a single collection at station 8 (9760 specimens, 13.2 ind. m⁻³).

In contrast, meroplankton exhibited very low abundances. The most representative taxa were zoeae of *Grimothea gregaria*, with 0.28% dominance (0.002, 0.001–0.02 ind. m⁻³; Table A2), cyphonauta larvae of bryozoans, with 0.20% dominance (0.008, 0.005–0.017 ind. m⁻³), and crustacean larvae in the mysis stage, with 0.10% dominance (0.005, 0.002–0.013 ind. m⁻³). In addition, the only representative of ichthyoplankton was a postflexion larva of the icefish *Champscephalus esox*, which constitutes the first record of an early life stage of this species

in the literature (The specimen is deposited in the Museo Nacional de Historia Natural, Santiago, Chile (MHNCL), under catalog number MHNCL 7737; Figure A1).

Mixed-level taxonomic richness ranged from 6 taxa at station E1 to 15 taxa at E2. Simpson diversity varied between 0.4 (E8) and 0.8 (E7), showing an increase toward the inner part of the bay (Figure 2A). The highest abundances ($>1000 \text{ ind. m}^{-2}$) were concentrated at stations most exposed to the Whiteside Channel (E8, E1, and E3), while the lowest abundances ($<100 \text{ ind. m}^{-2}$) occurred in scattered sites within Inútil Bay (E6, E4, E10, and E7; Figure 2B). Evenness (J') fluctuated between 0.41 (E8) and 0.89 (E6), mirroring the pattern of Simpson diversity. Stations in the central-northern sector of the bay showed the highest levels of uniformity (>0.8) and also the greatest diversity values (Figure 2C,D).

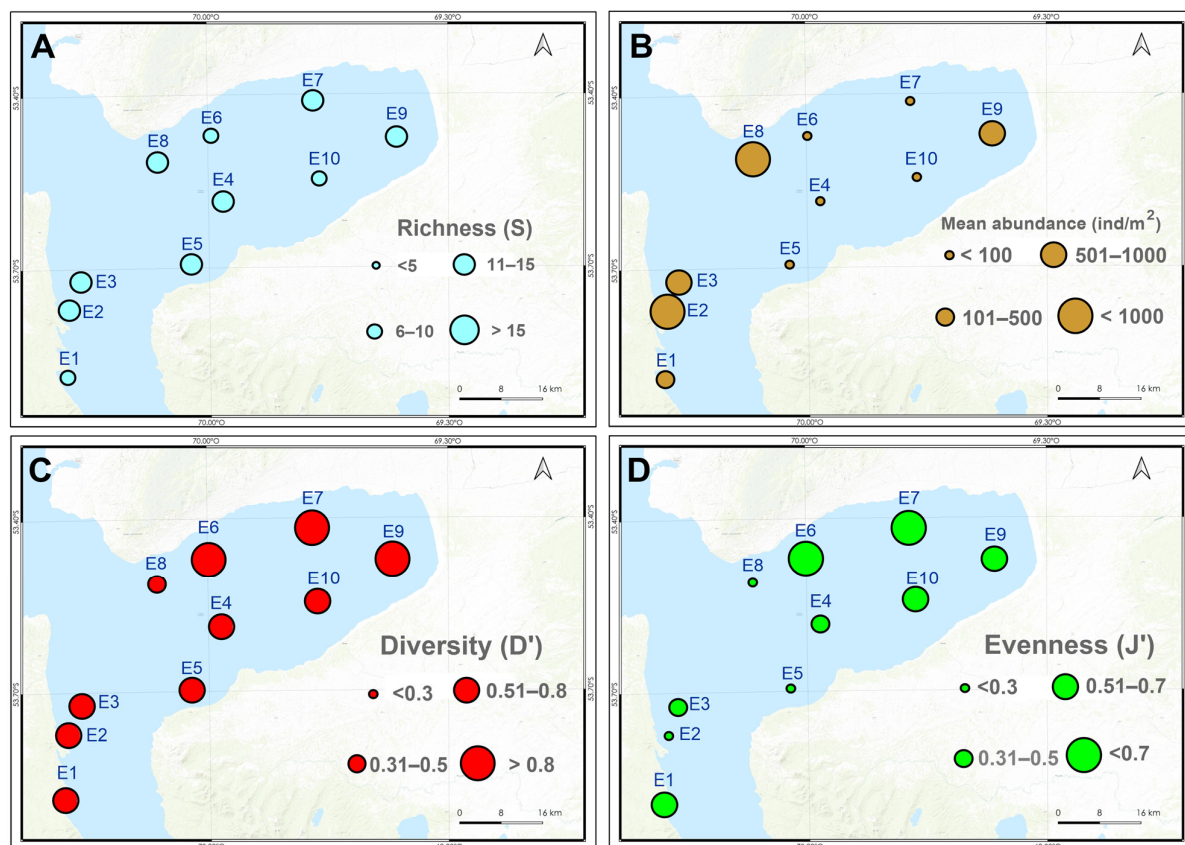


Figure 2. Characteristics of the zooplankton assemblage across sampling stations. (A). Mixed-level taxonomic richness, (B). Number of individuals (ind. m^{-2}), (C). Simpson diversity, (D). Pielou's evenness.

The non-metric multidimensional scaling (nMDS) analysis identified three main groups with 60% similarity. Stations located outside the bay were more similar to each other and to those situated at the southern margin of the bay's entrance. In contrast, stations at the northern margin and the head of the bay showed higher similarity among themselves. Station E8 stood out as the most dissimilar, segregating primarily due to the high abundance of ostracods (Figure 3A,B). The assemblages did not show significant differences associated with areas (PERMANOVA $\text{pseudo-}F = 1.799$, $p = 0.0745$). The abundance of copepods such as *Clausocalanus arcuicornis* and *Clausocalanus brevipes* contributed significantly to the differentiation of these stations, while species such as *Themisto gaudichaudii*, *Candacia* sp., and *Subeucalanus* sp. showed distribution patterns associated with the more exposed stations (Figure 3C,D).

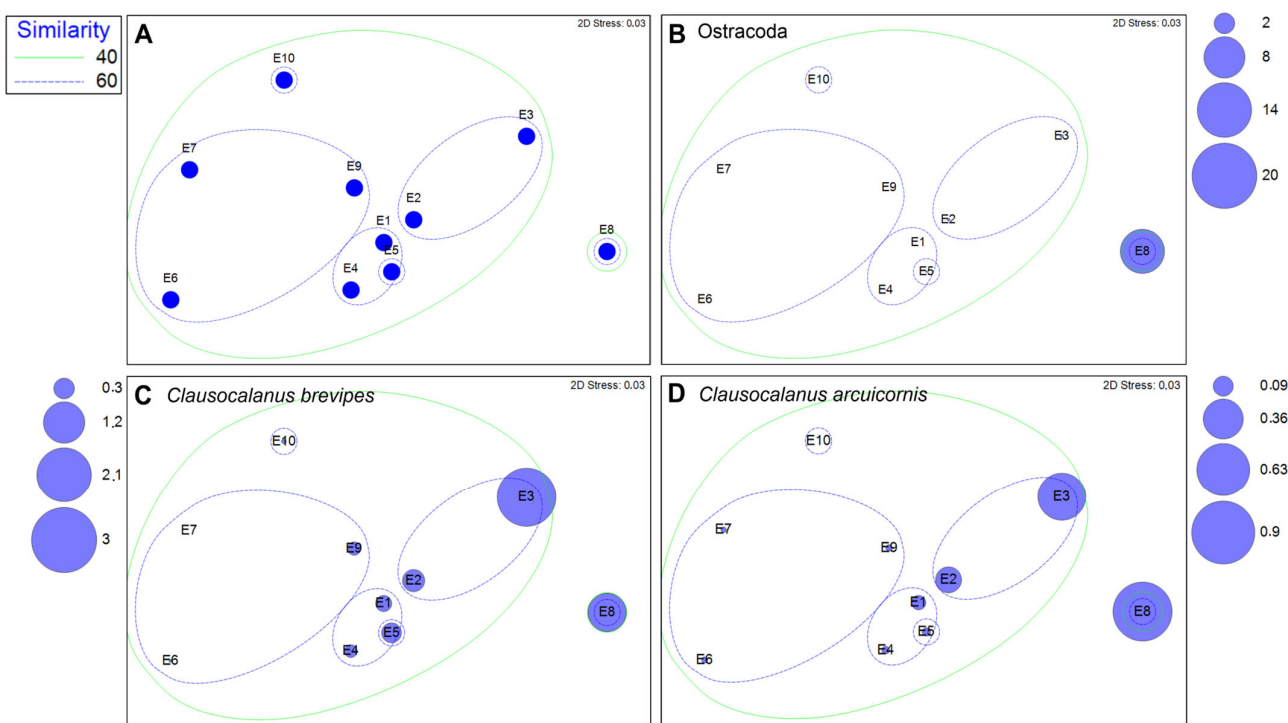


Figure 3. Non-metric multidimensional scaling (nMDS) of zooplankton taxa abundances in Inútil Bay. Abundances were standardized to individuals per cubic meter (ind. m^{-3}) and log-transformed [$\log_{10}(x + 1)$]. Bubble size is proportional to the abundance of each taxon at each station; the values in the side legend indicate abundance (ind. m^{-3}). Contours represent Bray–Curtis similarity groups obtained through hierarchical cluster analysis (outer: 40%; inner: 60%). A contour enclosing a single station indicates a unique group (singleton) at that similarity level. Distribution of the species contributing most to the assemblage structure: (A) All stations, (B) Ostracoda, (C) *Clausocalanus brevipes* (Copepoda), (D) *Clausocalanus arcuicornis* (Copepoda).

3.2. Megabenthic Assemblages

A total of 61 taxonomic groups were identified; of the total taxa, 32 were sessile and 29 non-sessile, including 12 Crustacea, 11 Mollusca, and 9 Echinodermata (Table A3). The squat lobster *Grimothea gregaria* was the most dominant species (Figure 4B), representing 55.5% of total abundance (median, 25–75% quartiles; 375.0, 185.25–641.0 $\text{ind. 10 m} \cdot \text{min}^{-1}$). The scallop *Zygochlamys patagonica* ranked second, accounting for 16.4% of dominance (165.0, 8.0–289.5 $\text{ind. 10 m} \cdot \text{min}^{-1}$), followed by the tube-dwelling polychaete *Chaetopterus variopedatus* with 7% dominance (42.5, 3.25–90.25 $\text{ind. 10 m} \cdot \text{min}^{-1}$; Table A3).

The spatial pattern showed a decline in alpha diversity indices toward the more sheltered and inner sector of the bay. Mixed-level taxonomic richness ranged from 11 to 28 taxa, with the highest values recorded at stations E1 (27 taxa), E5 (26), E4 (25), and E2 (23), located in the Whiteside Channel and the western margin of Inútil Bay (Figure 5A). In contrast, the innermost stations, such as E8, E9, and E10, exhibited the lowest richness (11–15 taxa). Similarly, the highest abundances (>1000 individuals) were concentrated at stations most exposed to the channel (E1–E5), while E8 and E9 registered the lowest abundances (<500 individuals; Figure 5B). Simpson diversity was highest at stations E1, E4, E5, E6, and E10 ($D' > 0.5$), reflecting more balanced communities, whereas lower values ($D' < 0.5$) were observed at E3, E7, and E9, indicating dominance by a few species (Figure 5C). Overall, diversity also decreased toward the inner sector of the bay. Evenness (J') showed relatively homogeneous values among stations, ranging from 0.13 (E2, E3) to 0.28 (E4; Figure 5D).

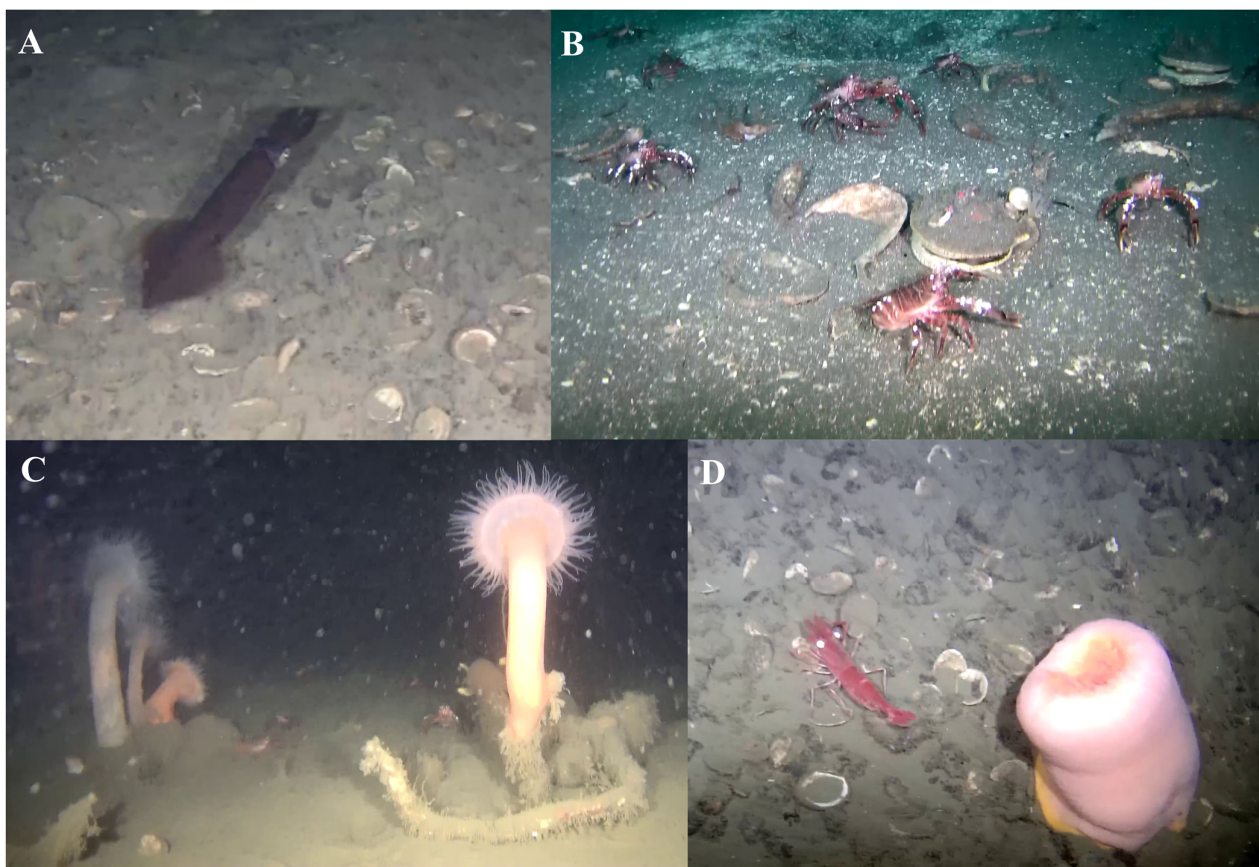


Figure 4. Remotely operated vehicle (ROV) images of the benthic community. (A). Specimen of *Doryteuthis gahi*; (B). Aggregation of *Grimothea gregaria*; (C). Colonies of *Actinostola* sp.; (D). Specimen of Caridea and Actinaria.

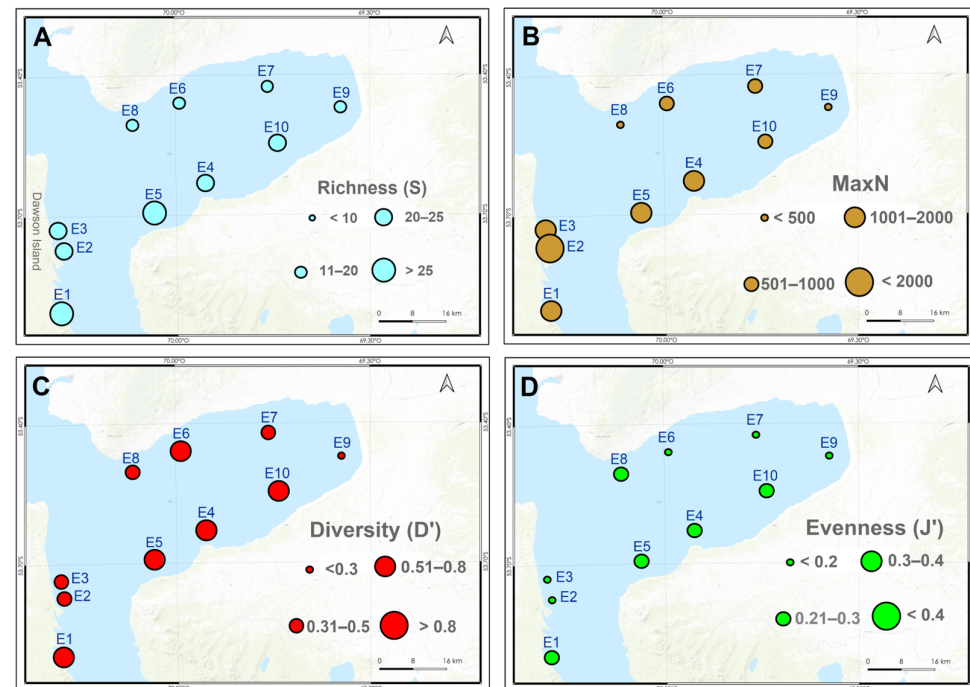


Figure 5. Characteristics of the megabenthic assemblage across sampling stations. (A). Mixed-level taxonomic richness, (B). Number of individuals (MaxN , $10 \text{ m} \cdot \text{min}^{-1}$), (C). Simpson diversity (H'), (D). Pielou's evenness (J').

The non-metric multidimensional scaling (nMDS) analysis identified three main clusters with 60% similarity. Stations located outside the bay were more similar to each other and to those at the southern entrance. In contrast, stations E6, E7, and E9, situated on the northeastern margin of the bay, formed a distinct group. Station E8 was segregated from the rest, primarily due to the low abundances of *Grimothea gregaria* and *Chaetopterus variopedatus*, together with the absence of *Zygochlamys patagonica* (Figure 6B). Although variations in the occurrence of these species were observed between the inner bay and outer areas, no statistically significant differences were detected in assemblage composition PERMANOVA pseudo- $F = 1.432$, $p = 0.186$.

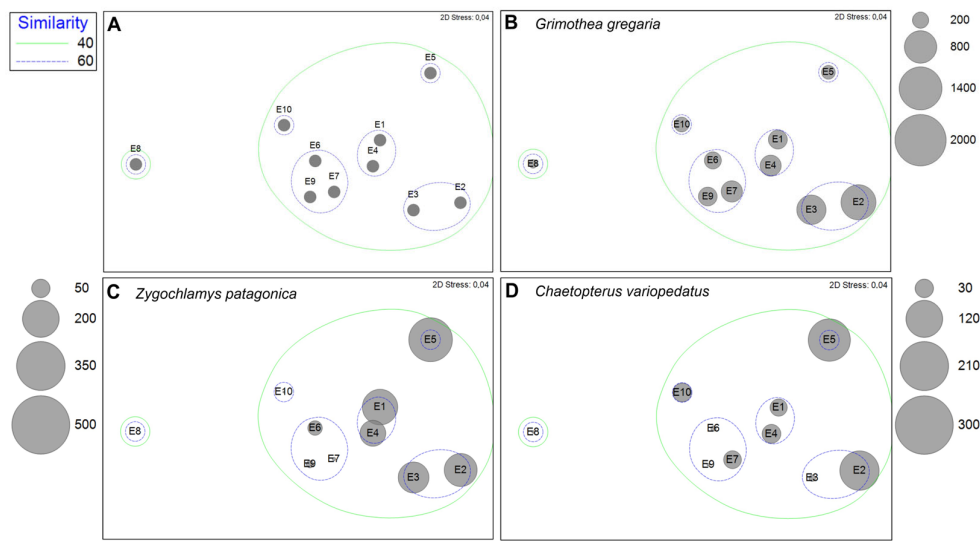


Figure 6. Non-metric multidimensional scaling (nMDS) of the abundance of soft-bottom megabenthic taxa in Inútil Bay. Abundances were expressed as Nmax (maximum counts per taxon across transects). Bubble size is proportional to taxon abundance at each station; side legend values indicate Nmax counts. Contours denote Bray–Curtis similarity groups derived from hierarchical clustering (outer: 40%; inner: 60%). A contour enclosing a single station indicates a singleton group at that similarity threshold. Distribution of the species contributing most to the assemblage structure: (A) All stations, (B) *Grimothea gregaria*, (C) *Zygochlamys patagonica*, (D) *Chaetopterus variopedatus*.

3.3. Macrofauna Assemblages

A total of 146 taxa were recorded, distributed across 10 phyla. The most diverse and abundant group was Annelida, with 80 taxa (median = 2318.2 ind. m^{-2}), followed by Crustacea (31 taxa; median = 224.45 ind. m^{-2}) and Mollusca (23 taxa; median = 207.7 ind. m^{-2}). Within Annelida, the assemblage was dominated by *Aricidea* spp., contributing 19.6% of the total abundance (median = 348.4; 25–75% quartiles: 58.6–842.5 ind. m^{-2} ; Table A4), followed by *Tharyx* spp. with 13.5% (244.6; 22.5–529.3 ind. m^{-2}) and *Aphelochaeta* spp. with 6.6% (13.4; 6.7–469 ind. m^{-2}). Among Crustacea, *Monocorophium* sp. was the most representative taxon, accounting for 1.8% of the total abundance (6.7; 6.7–13.4 ind. m^{-2}), while *Fuegiphoxus* sp. and *Urothoe falcata* reached 0.26% (53.6; 6.7–33.5 ind. m^{-2}) and 0.23% (6.7; 6.7–33.5 ind. m^{-2}), respectively. In Mollusca, the dominant species was *Thyasira* sp., contributing 3.9% (26.8; 12.8–368.5 ind. m^{-2}), followed by *Pseudoneilonella* sp. with 1.3% (26.8; 13.4–110.6 ind. m^{-2}) and *Yoldiella* sp. with 1.1% (30.2; 5.0–139.0 ind. m^{-2}). Additionally, the brachiopod *Magellania venosa* reached 4.1% dominance (77.1; 3.5–244.6 ind. m^{-2}), while *Nematoda* represented 10.4% of the assemblage (50.3; 26.8–335 ind. m^{-2}), highlighting its importance in the innermost and more protected stations.

The spatial pattern showed a decrease in alpha indices toward the more protected and inner sector of Inútil Bay. Mixed-level taxonomic richness (S) ranged from 25 to 61 taxa, with the highest values at E1 (61 taxa), E2 (41), and E3 (39). In contrast, the innermost

stations, such as E6 (25), E7 (28), and E8 (29), exhibited the lowest richness (Figure 7A). Total abundance ranged from 978 to 5206 ind. \cdot m $^{-2}$, with maxima at E1 (5206 ind. \cdot m $^{-2}$) and E8 (4663), despite their differences in richness, whereas E5 (978) and E2 (1206) recorded the lowest densities (Figure 7B). Simpson diversity index (D') remained high, with values close to 1 at almost all stations (>0.79 ; Figure 7C), reflecting dominance by few species (Figure 7C). Evenness (J') followed this pattern, with higher values at E2 (0.6), E5 (0.5), and E7 (0.5), and reduced values at E1, E6, and E8 (0.3; Figure 7D).

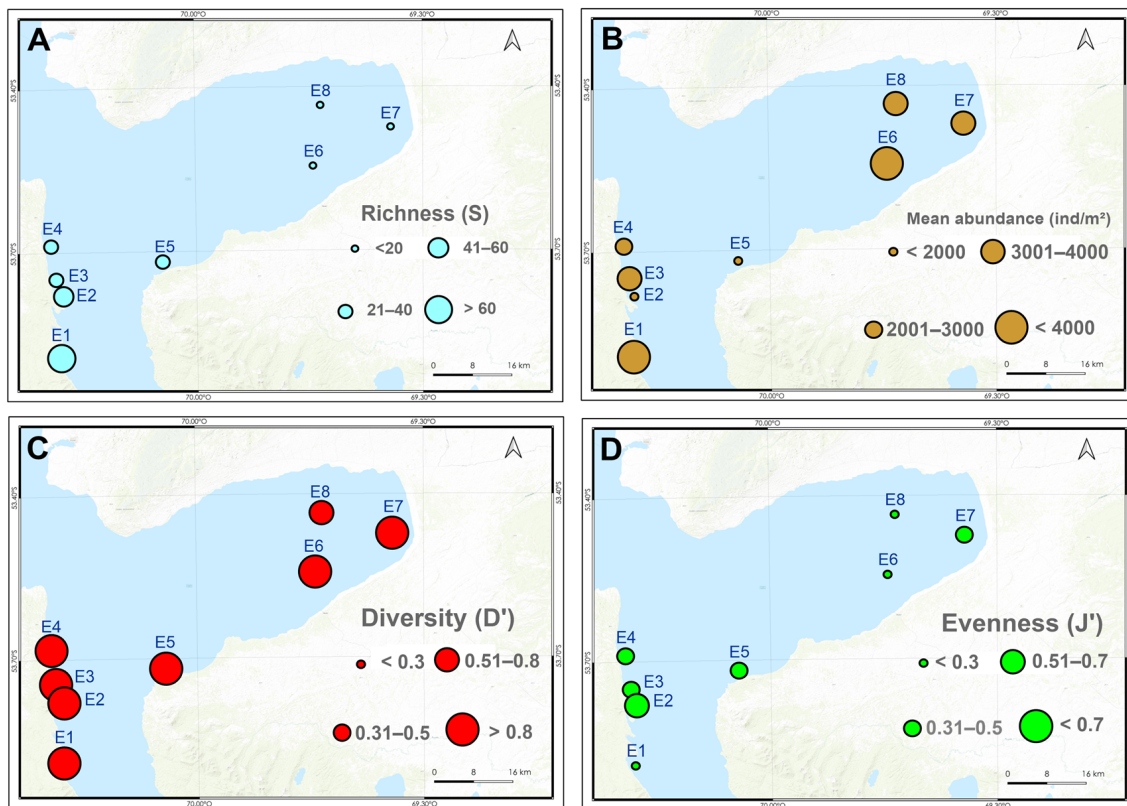


Figure 7. Characteristics of the soft-bottom macrobenthic assemblage among sampling stations. **(A)**. Mixed-level taxonomic richness, **(B)**. Number of individuals (ind. \cdot m $^{-2}$), **(C)**. Simpson diversity, **(D)**. Pielou's evenness (J').

The NMDS analysis (stress = 0.02) revealed a clear spatial differentiation in the composition and abundance of dominant taxa among the sampled stations, with well-defined groupings at similarity levels of 60% (blue dashed lines) and 40% (green lines; Figure 8A). The most exposed stations of the bay (E1–E4) clustered with high similarity ($\geq 60\%$), characterized by high abundances of the polychaete *Tharyx* sp. (especially in E1; Figure 8C) and the brachiopod *Magellania venosa*. In these stations, *Aricidea* sp., *Capitella* sp., and Nematoda were scarcely represented. In contrast, the more sheltered and inner stations (E6–E8) formed a well-defined cluster at $\geq 60\%$ similarity, dominated by *Capitella* sp. and *Aricidea* sp. (Figure 8B–D), both reaching maximum abundances at E6 and E8, along with a high representation of Nematoda (Figure 8F), suggesting more restricted or environmentally stressed conditions. Station E5 did not cluster with any other under the similarity thresholds considered, indicating a unique faunal composition and possibly a distinct or transitional environmental condition. Significant differences were detected between assemblages at stations located outside and inside the bay (PERMANOVA, $\text{pseudo-}F = 4.013$, $p = 0.0186$). Dissimilarity was mainly driven by *Tharyx* spp., *Magellania venosa*, and *Pholoe* sp. (SIMPER, Table 1).

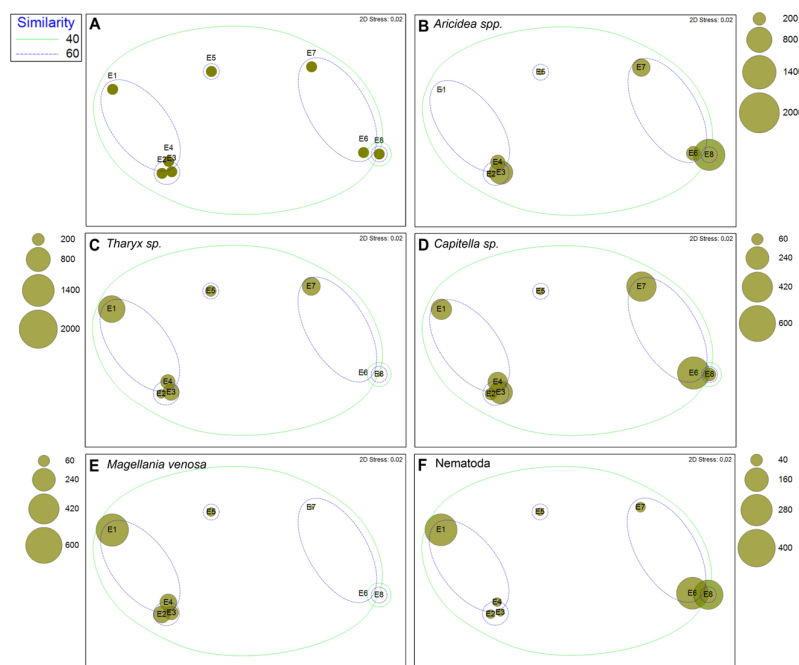


Figure 8. Non-metric multidimensional scaling (nMDS) of the abundance of soft-bottom macrobenthic taxa in Inútil Bay. Abundances were standardized to individuals per square meter (ind. m^{-2}) and fourth-root transformed ($x^{0.25}$). Bubble size is proportional to taxon abundance at each station; side legend values indicate abundance (ind. m^{-2}). Contours denote Bray–Curtis similarity groups from hierarchical clustering (outer: 40%; inner: 60%). A contour enclosing a single station indicates a singleton group at that similarity threshold. Distribution of the species contributing most to the assemblage structure: (A) All stations, (B) *Aricidea* spp. (Polychaeta), (C) *Tharyx* sp. (Polychaeta), (D) *Capitella* sp. (Polychaeta), (E) *Magellania venosa* (Brachiopoda), (F) Nematoda.

Table 1. Similarity Percentage (SIMPER) analysis results for the comparison of dissimilarity (Overall average dissimilarity = 60.03%) of the benthic macrofauna contributing >1.5% to the total dissimilarity inside and outside Inútil Bay, Tierra del Fuego.

Taxa	Av. Dissim	Contrib. %	Cumulative %	Mean Outside	Mean Inside
<i>Tharyx</i> spp.	1.568	2.612	2.612	1.41	4.56
<i>Magellania venosa</i>	1.41	2.348	4.96	3.49	0.536
<i>Pholoe</i> sp.	1.262	2.102	7.063	0	2.55
<i>Kirkegaardia</i> spp.	0.9944	1.657	8.719	4.4	2.78
<i>Lepidozona</i> sp.	0.9777	1.629	10.35	2.01	0
<i>Levinsenia</i> sp.	0.9569	1.594	11.94	3.46	5.17
<i>Yoldiella</i> sp.	0.9061	1.509	13.45	2.22	0.902
<i>Eunireis patagonica</i>	0.9034	1.505	14.96	0	1.82
Nematoda	0.9006	1.5	16.46	2.77	4.19

4. Discussion

The present study is not only the first to provide high-resolution biological information from Inútil Bay but also one of the few to encompass both benthic and zooplanktonic communities in Patagonian bays. This information was derived from the analysis of high-resolution data on taxonomic composition and abundance obtained through simultaneous sampling of mesozooplankton and benthic fauna in Inútil Bay and adjacent areas. The combined use of dredging and ROV-based observations, an approach scarcely applied in the region, allowed for a more comprehensive characterization of benthic assemblages, expanding habitat coverage and reducing the likelihood of underestimating biodiversity. This complementary approach proved particularly valuable for detecting both highly

mobile species, which typically evade passive sampling, and those associated with or buried in the substrate [15].

The mesozooplankton community exhibited low abundance but higher diversity and evenness in the northeastern sector of the bay; however, no clear zonation pattern was observed. The mixed-level taxonomic richness totaled 32 taxa, exceeding the 21 taxa previously reported during summer by Zagami et al. (2011) [11]. As in other Patagonian areas, the community was characterized by low diversity and marked dominance [16,50–52]. Copepods, mostly of sub-Antarctic distribution, dominated the assemblage, with *Clausocalanus brevipes* (median: 0.220 ind. m^{-3}) as the most abundant holoplanktonic species, typical of coastal systems of Patagonia and Antarctica [52,53]. Other species included *Clausocalanus arcuicornis* (median: 0.017 ind. m^{-3}) and *Acartia* sp. (median: 0.028 ind. m^{-3}). In addition, copepods of the order Monstrilloidea were recorded, parasites of polychaetes and bivalves in early stages (nauplius to juvenile), whose adults detach from the host to reproduce in the water column [54]. Among these, *Monstrilla* sp. and *Cymbasoma* sp. were detected, the latter with only a few records in southern Patagonia [55]. Other groups, such as ostracods and siphonophores, reached high densities at a single station, likely favored by local factors such as vertical mixing [56]. Although previous studies proposed that the Magdalena Sound–Puerto del Hambre–Paso Ancho sub-basin supports relatively stable zooplankton assemblages, the dominant species in this study differed from earlier reports [53,57], suggesting that Inútil Bay may exhibit oceanographic conditions that promote distinct planktonic communities. Regarding ichthyoplankton, previous studies [9] reported only fish eggs and no larvae [10], whereas in the present study a single early stage was recorded: a postflexion larva of *Champscephalus esox*, representing the first record of a larval stage for this little-known species.

In contrast, both megabenthic and macrobenthic assemblages showed the highest taxonomic richness, diversity, and evenness outside Inútil Bay and at stations more exposed to the Whiteside Channel. These spatial patterns appear to be linked to environmental differences associated with exposure, bathymetry, and sediment type [28,50,57], together with functional traits of the taxa (e.g., trophic preferences, dispersal strategies) [58,59] that enhance settlement success in certain substrates over others. Research on benthic communities in Inútil Bay has been scarce and intermittent, beginning in the 1990s with one of the first analyses of sublittoral macrobenthos, focused exclusively on Polychaeta, with a total of 37 species [14]. Almost a decade later, the first study including the entire macrofaunal assemblage broadened the taxonomic scope, recording 173 taxa [8]. More recently, the macrobenthic community of Inútil Bay and its functional connectivity with Almirantazgo Sound were described in detail [13]. In the present study, 211 benthic taxa typical of soft-bottom habitats were identified, including macrofaunal and megafaunal species, some of high ecological relevance as habitat formers (*Chaetopterus variopedatus*, *Apomatus* sp., *Magellania venosa*, *Mytilus* sp.), and others of commercial value for local communities (*Lithodes santolla*, *Zygochlamys patagonica*, *Grimothea gregaria*). The latter forms large aggregations [60], that have emerged as a potential fishery resource; however, their harvest also involves at least 44 associated species [61], largely composed of filter feeders, suspension feeders, and detritivores [22].

Previous studies reported lower benthic abundances compared to those observed here. Gambi and Mariani (1999) [14] found an average of 184 individuals considering only polychaetes, dominated by *Prionospio (Minuspio)* sp. (24 ind.), *Onuphis pseudoiridescens* (21 ind.), and *Ninoe falklandica* (19 ind.). Thatje and Brown (2009) [15] estimated mean densities of 1287 ind. m^{-2} , with Polychaeta as the dominant group at all stations, particularly *Aricidea* sp. 1 (604 ind. m^{-2}), *Caulieriella* sp. (480 ind. m^{-2}), *Minuspio patagonico* (438 ind. m^{-2}), and *Tharyx* sp. (386 ind. m^{-2}). Among mollusks, *Mysella* sp. (333 ind. m^{-2}),

Yoldiella valettei (126 ind. m^{-2}), and *Antistreptus magellanicus* (83 ind. m^{-2}) were recorded, while Amphipoda included *Heterophoxus videns* and *Urothoe falcata*. More recently, Jara et al. (2024) [16] reported a mean abundance of 888.9 ± 26.8 ind. m^{-2} , with Polychaeta as the most numerous group (440.0 ± 89.0 ind. m^{-2}), followed by Mollusca (243.4 ± 304.7 ind. m^{-2}) and Arthropoda (93.8 ± 75.4 ind. m^{-2}). By comparison, the present study recorded a median of 3283 ind. m^{-2} , substantially higher than previous estimates, while maintaining the dominance of polychaetes, particularly *Aricidea* spp. and *Tharyx* spp., already recognized as dominant taxa and continuing to play a structural role in the macrobenthos of Inútil Bay. The higher benthic abundances observed in this study may be attributed to differences in sampling design and local environmental conditions rather than to real temporal variations. While the studies by Gambi and Mariani (1999) [14] and Thatje and Brown (2009) [15] were conducted in summer, the present sampling was carried out in winter (July 2024). Factors such as the use of a finer mesh (0.5 mm), a larger sampling area, and standardized replication could explain the higher abundances recorded. Their spatial distribution appears to be driven by bathymetric and sedimentological variability, unlike other benthic communities in the region.

Sampling also revealed a high abundance and diversity of adult benthic invertebrates but a scarce representation of early meroplanktonic stages, which likely reflects seasonal reproductive patterns typical of austral winter conditions. Among the main representatives were bryozoan cyphonaut larvae and *Grimothea gregaria* zoeae at different stages, taxa commonly reported and often dominant in coastal meroplankton during the austral winter in southern Patagonia [53,60,61]. However, no polychaete larvae were recorded, in contrast to the high abundance and taxonomic richness of this group in the local benthos. A likely explanation is that many benthic species exhibit strongly seasonal reproductive cycles, concentrating larval release in austral spring and summer, synchronized with oceanographic processes that ensure food availability during the planktonic phase [62]. The scarcity of meroplankton, together with the absence of emergent benthos at shallow stations (<75 m), suggests limited benthopelagic interaction during the austral winter in Inútil Bay, as reflected by the low representation of larval stages in the plankton relative to the high abundance and diversity of adult invertebrates in the benthos. In this context, anthropogenic impacts during colder periods, when larval recruitment is limited, could have significant consequences for community structure and dynamics.

Although the area currently shows some degree of human disturbance, its proximity to aquaculture-suitable areas, the growing fishing effort in the region [63], interest in large-scale energy projects [64,65], and the development of unregulated tourism [66] expose it to considerable risks of ecological degradation. These activities may cause habitat loss and fragmentation [67,68], the introduction of invasive species [69], pollution [70], overexploitation of resources, and disruption of key ecological processes, affecting both benthic and pelagic communities.

A comprehensive assessment of biodiversity in Inútil Bay is therefore essential to establish conservation baselines, implement adaptive management, and prevent irreversible impacts. Documenting and understanding local biodiversity thus becomes a critical step toward recognizing the bay as a conservation priority and ensuring the provision of socio-ecosystem services.

5. Conclusions

This study provides the first integrated characterization of the marine communities of Inútil Bay, revealing high biodiversity and a marked spatial structure. A total of 211 benthic and 32 zooplanktonic taxa were recorded, dominated by polychaetes (*Aricidea* spp., *Tharyx* spp.) and copepods (*Clausocalanus* spp.). Macrobenthic assemblages showed significant differ-

ences between inner and outer stations of the bay. Inner areas exhibited lower richness and diversity, whereas sites more exposed to the Whiteside Channel harbored more diverse and even communities. The low presence of larval stages in the plankton suggests weak benthopelagic connectivity during the austral winter, associated with reduced seasonal reproductive activity. Inútil Bay retains high ecological value but faces increasing pressures from human activities.

For future studies, it would be valuable to repeat surveys with a comparable design during other seasons of the year to contrast seasonal patterns of biodiversity and benthopelagic connectivity. Additionally, incorporating oceanographic and sedimentological data would allow for a more precise understanding of the relationships between biological composition, ecological indices, and the environmental conditions structuring the marine communities of Inútil Bay.

Author Contributions: M.F.L. and M.H.; Methodology, B.R.-S. and M.H.; Software, I.G.; Validation, A.M., M.F.L., J.P.-S., I.G. and M.H.; Formal Analysis, B.R.-S.; Investigation, J.P. and M.H.; Resources, J.P., I.G. and M.H.; Data Curation, A.M., J.P., D.P., J.P.-S., K.S., I.G. and F.S.O.; Writing—Original Draft Preparation, B.R.-S., A.M., M.F.L., D.P. and M.H.; Writing—Review & Editing, B.R.-S., A.M., M.F.L. and M.H.; Visualization, B.R.-S.; Supervision, M.H.; Project Administration, M.H. All authors have read and agreed to the published version of the manuscript.

Funding: This research was funded by Fundación Rewilding Chile.

Institutional Review Board Statement: Fieldwork and the collection of zooplankton and benthic macrofauna were authorized by the Chilean Fisheries Service under a Technical Memorandum (R. EX. N°E-2021-670 SUBPESCA; Code: 29228521125; Date 1 December 2021).

Data Availability Statement: Data are contained within the manuscript.

Acknowledgments: This work was made possible by Fundación Rewilding Chile, a Chilean non-profit financially supported by an extensive philanthropic network.

Conflicts of Interest: The authors declare no conflicts of interest.

Appendix A

Table A1. Depth of sampling stations in Inútil Bay and adjacent areas (2024). The figure indicates the towing depth during mesozooplankton hauls, the recording depth used for megabenthos analysis based on ROV observations, and the depth of the site where sediment dredging was conducted for macrobenthos analyses.

Zooplankton Station	Depth (m)	Megabenthos Station	Depth (m)	Macrobenthos Station	Depth (m)
E1	100	E1	25–26	E1	28
E2	80	E2	29–27	E2	28
E3	85	E3	32–33	E3	30
E4	15	E4	23–24	E4	34
E5	75	E5	26–26	E5	26
E6	40	E6	64–65	E6	40
E7	25	E7	48–48	E7	27
E8	100	E8	151–139	E8	50
E9	10	E9	26–26		
E10	15	E10	37–37		

Table A2. Taxonomic composition, standardized abundances, and relative dominance of the zooplankton recorded in Inútil Bay, Strait of Magellan. Taxa are grouped into holoplanktonic and meroplanktonic forms. Abundances are standardized as number of individuals per cubic meter (ind. m^{-3}). Median, 25% quartile (25Q), and 75% quartile (75Q) values are shown for each taxon, together with their relative dominance (%) within the total zooplankton.

Holoplankton		Order	Taxon	Median	25Q	75Q	%
Phylum	Class						
Foraminifera	—	—	Foraminifera	0.013	0.007	0.019	0.099
Cnidaria	Hydrozoa	—	Siphonophora	0.012	0.00375	0.333	4.739
Cnidaria	Hydrozoa	—	Hydromedusae	0.007	0.007	0.007	0.028
Arthropoda	Copepoda	Calanoida	<i>Calanus</i> sp.	0.043	0.013	0.205	1.828
Arthropoda	Copepoda	Calanoida	<i>Paracalanus</i> sp.	0.280	0.087	0.282	2.476
Arthropoda	Copepoda	Calanoida	<i>Acartia</i> sp.	0.028	0.007	0.084	1.940
Arthropoda	Copepoda	Calanoida	<i>Clausocalanus arcuicornis</i>	0.017	0.0095	0.352	6.236
Arthropoda	Copepoda	Calanoida	<i>Clausocalanus brevipes</i>	0.220	0.078	0.828	20.800
Arthropoda	Copepoda	Calanoida	<i>Candacia</i> sp.	0.424	0.001	0.847	3.235
Arthropoda	Copepoda	Calanoida	<i>Centropages</i> sp.	0.006	0.001	0.010	0.042
Arthropoda	Copepoda	Calanoida	<i>Temora</i> sp.	0.017	0.017	0.017	0.065
Arthropoda	Copepoda	Calanoida	<i>Subeucalanus</i> sp.	0.197	0.003	0.391	1.501
Arthropoda	Copepoda	Monstrilloida	<i>Cymbasoma</i> sp.	0.002	0.001	0.045	0.184
Arthropoda	Copepoda	Monstrilloida	<i>Monstrilla</i> sp.	0.002	0.002	0.002	0.009
Arthropoda	Copepoda	Harpacticoida	<i>Alteutha</i> sp.	0.033	0.033	0.033	0.126
Arthropoda	Copepoda	Cyclopoida	<i>Oncaeia</i> sp.	0.003	0.003	0.003	0.013
Arthropoda	Eucarida	—	<i>Furcilia</i>	0.001	0.001	0.001	0.005
Arthropoda	Peracarida	Isopoda	Isopoda	0.002	0.002	0.002	0.008
Arthropoda	Peracarida	Amphipoda	<i>Themisto gaudichaudii</i>	0.022	0.012	0.039	1.048
Arthropoda	Peracarida	Amphipoda	Hyperiidae	0.001	0.001	0.001	0.005
Arthropoda	Peracarida	Amphipoda	Hyalellidae	0.001	0.001	0.001	0.005
Arthropoda	Ostracoda	—	Ostracoda	0.055	0.012	6.654	51.079
Arthropoda	Malacostraca	Decapoda	<i>Grimothea gregaria</i>	0.007	0.004	0.020	0.120
Chaetognatha	—	—	Chaetognatha	0.014	0.0035	0.373	2.930
Chordata	—	—	Appendicularia	0.028	0.0075	0.068	0.804
Meroplankton							
Bryozoa	—	—	<i>Cyphonauta</i> larvae	0.008	0.006	0.018	0.207
Mollusca	Bivalvia	—	<i>Bivalvia</i> larvae	0.004	0.004	0.004	0.014
Arthropoda	Malacostraca	Decapoda	<i>Mysis</i> larvae	0.005	0.002	0.013	0.102
Arthropoda	Malacostraca	Decapoda	<i>Zoea</i> <i>Grimothea gregaria</i>	0.003	0.001	0.020	0.282
Arthropoda	Malacostraca	Decapoda	<i>Zoea</i> <i>Pinnotheridae</i>	0.004	0.001	0.010	0.058
Arthropoda	Malacostraca	Decapoda	<i>Prezoea</i> I	0.002	0.002	0.002	0.008
Chordata	Actinopterygii	—	<i>Champscephalus esox</i> larvae	0.001	0.001	0.001	0.004

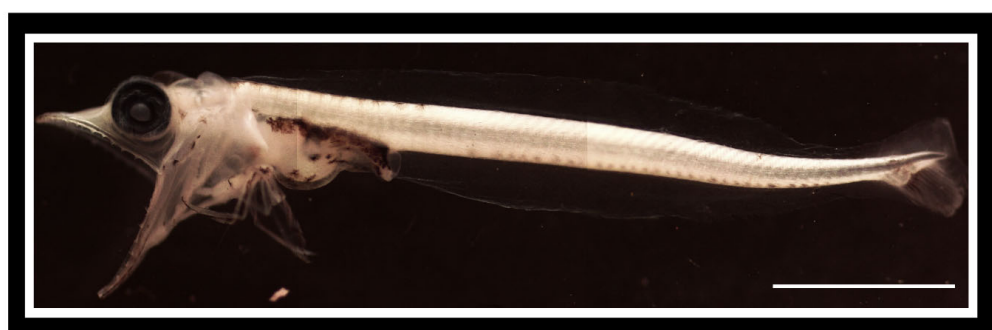


Figure A1. First record of an early life stage of the icefish *Champscephalus esox* in the literature. Inútil Bay, July 2024. (Scale: 0.5 mm). Deposited in the Museo Nacional de Historia Natural, Santiago, Chile (number: MNHN-ICT 7737).

Table A3. Taxonomic composition, standardized abundances, and relative dominance of megabenthic organisms recorded through ROV imagery in Inútil Bay, Strait of Magellan. Abundances are expressed as MaxN per $10\text{ m}\cdot\text{min}^{-1}$. For each taxon, median values, lower quartile (25Q), and upper quartile (75Q) are shown, together with the percentage of relative dominance (%) with respect to the total assemblage.

Phylum	Class	Order	Taxa	Median	25Q	75Q	%
Porifera	Demospongiae	Poecilosclerida	<i>Amphilectus americanus</i>	1.0	1.0	19.0	0.226
Porifera	Demospongiae	Hadromerida	<i>Cliona chilensis</i>	2.0	2.0	2.0	0.022
Porifera	Demospongiae	Poecilosclerida	<i>Mycale magellanica</i>	1.0	1.0	1.0	0.011
Porifera	Demospongiae	Hadromerida	<i>Polymastia</i> sp.	1.0	1.0	1.0	0.011
Porifera	Demospongiae	—	Porifera	28.0	5.0	56.25	6.989
Porifera	Demospongiae	Poecilosclerida	<i>Tedania mucosa</i>	1.0	1.0	1.0	0.011
Porifera	Demospongiae	Hadromerida	<i>Tethya papillosa</i>	1.0	1.0	1.0	0.011
Cnidaria	Anthozoa	Actiniaria	Actiniaria	3.5	3.0	4.0	0.075
Cnidaria	Anthozoa	Actiniaria	<i>Actinostola</i> sp.	2.0	1.0	35.0	0.409
Cnidaria	Anthozoa	Alcyonacea	<i>Alcyonium</i> sp.	3.0	2.0	5.0	0.108
Cnidaria	Anthozoa	Scleractinia	<i>Desmophyllum dianthus</i>	1.0	1.0	1.0	0.011
Cnidaria	Anthozoa	Scleractinia	Hexacorallia	1.0	1.0	3.0	0.441
Cnidaria	Hydrozoa	Anthoathecata	Hydrozoa	11.0	6.0	32.0	2.129
Annelida	Polychaeta	Sabellida	<i>Apomatus</i> sp.	1.0	1.0	6.0	0.086
Annelida	Polychaeta	Terebellida	<i>Chaetopterus variopedatus</i>	42.5	3.25	90.25	7.044
Annelida	Polychaeta	—	Polychaeta	2.0	1.0	13.0	0.527
Mollusca	Gastropoda	Neogastropoda	<i>Adelomelon ancilla</i>	1.0	1.0	1.0	0.011
Mollusca	Bivalvia	Venerida	<i>Ameghinomya antiqua</i>	2.0	1.0	25.0	0.581
Mollusca	Bivalvia	Venerida	Bivalvia	4.0	3.0	5.0	0.086
Mollusca	Gastropoda	Trochida	<i>Calliostoma consimilis</i>	1.0	1.0	1.0	0.011
Mollusca	Cephalopoda	Teuthida	Cephalopoda	1.0	1.0	1.0	0.011
Mollusca	Cephalopoda	Teuthida	<i>Doryteuthis gahi</i>	1.0	1.0	1.0	0.011
Mollusca	Gastropoda	Lepetellida	<i>Fissurella</i> sp.	2.0	2.0	2.0	0.022
Mollusca	Gastropoda	—	Gastropoda	2.0	1.0	3.0	0.065
Mollusca	Gastropoda	Heterobranchia	Heterobranchia	1.0	1.0	1.0	0.022
Mollusca	Bivalvia	Mytilida	<i>Mytilus</i> sp.	1.0	1.0	3.0	0.054
Mollusca	Bivalvia	Pectinida	<i>Zygochlamys patagonica</i>	165.0	8.0	289.5	16.357
Bryozoa	Gymnolaemata	Cheilostomatida	<i>Aspidostoma giganteum</i>	2.0	2.0	2.0	0.022
Bryozoa	Gymnolaemata	Cheilostomatida	<i>Bryozoa</i> sp.	3.5	1.5	4.0	0.344
Bryozoa	Gymnolaemata	Cheilostomatida	<i>Carbasea ovoidea</i>	7.0	3.75	17.75	0.699
Bryozoa	Gymnolaemata	Cheilostomatida	<i>Cellaria</i> sp.	1.5	1.0	2.75	0.075
Arthropoda	Malacostraca	Sessilia	<i>Austromegabalanus psittacus</i>	21.0	21.0	21.0	0.226
Arthropoda	Malacostraca	Caridea	Caridea	3.0	1.5	14.0	0.366
Arthropoda	Malacostraca	Sessilia	<i>Cirripedia</i> sp.	2.0	1.0	154.0	1.688
Arthropoda	Malacostraca	Decapoda	Decapoda	2.0	1.0	6.0	0.280
Arthropoda	Malacostraca	Decapoda	<i>Euryopodius latreillii</i>	3.0	1.0	6.0	0.237
Arthropoda	Malacostraca	Decapoda	<i>Grimothea gregaria</i>	375.0	185.25	641.0	55.490
Arthropoda	Malacostraca	Decapoda	<i>Lithodes santolla</i>	1.5	1.0	2.0	0.032
Arthropoda	Malacostraca	Decapoda	<i>Lophon proximum</i>	11.0	1.0	21.0	0.237
Arthropoda	Malacostraca	Decapoda	<i>Metacarcinus edwardsii</i>	1.0	1.0	1.0	0.011
Arthropoda	Malacostraca	Decapoda	<i>Nauticaris magellanica</i>	1.0	1.0	1.0	0.011
Arthropoda	Malacostraca	Decapoda	<i>Pagurus</i> sp.	1.0	1.0	1.0	0.011
Arthropoda	Malacostraca	Decapoda	<i>Pseudocorynites sicarius</i>	2.0	2.0	7.0	0.001
Echinodermata	Echinoidea	Arbacioida	<i>Arbacia dufresnii</i>	5.5	1.75	37.0	0.634

Table A3. Cont.

Phylum	Class	Order	Taxa	Median	25Q	75Q	%
Echinodermata	Astroioidea	Valvatida	Astroioidea	2.0	1.0	5.25	0.118
Echinodermata	Astroioidea	Valvatida	<i>Cosmasterias lurida</i>	10.5	3.5	25.0	1.592
Echinodermata	Astroioidea	Valvatida	<i>Glabraster antarctica</i>	1.0	1.0	1.0	0.011
Echinodermata	Holothuroidea	Dendrochirotida	Holothuroidea	2.5	1.25	5.25	0.129
Echinodermata	Astroioidea	Paxillosida	<i>Labidiaster radiosus</i>	4.5	4.0	5.0	0.097
Echinodermata	Astroioidea	Valvatida	<i>Odontaster penicillatus</i>	1.0	1.0	1.0	0.011
Echinodermata	Ophiuroidea	Ophiurida	<i>Ophiura</i> sp.	1.0	1.0	1.0	0.011
Echinodermata	Astroioidea	Valvatida	<i>Patiria chilensis</i>	1.0	1.0	1.0	0.011
Chordata	Ascidacea	Stolidobranchia	Ascidacea	4.0	1.25	8.0	0.613
Chordata	Ascidacea	Stolidobranchia	<i>Cnemidocarpa</i> sp.	3.0	3.0	3.0	0.032
Chordata	Ascidacea	Aplousobranchia	<i>Didemnum studeri</i>	1.0	1.0	57.25	1.043
Chordata	Ascidacea	Aplousobranchia	<i>Distaplia cylindrica</i>	1.0	1.0	1.0	0.032
Chordata	Ascidacea	Stolidobranchia	<i>Pyura legumen</i>	3.5	1.0	6.0	0.001
Chordata	Ascidacea	Aplousobranchia	<i>Sycozoa</i> sp.	2.0	2.0	2.0	0.022
Chordata	Ascidacea	Aplousobranchia	<i>Sycozoa gaimardi</i>	5.0	1.0	9.0	0.258
Chordata	Ascidacea	Aplousobranchia	<i>Sycozoa sigillinaoides</i>	7.5	1.0	14.0	0.108

Table A4. Taxonomic composition, standardized abundances, and relative dominance of benthic macrofauna from soft-bottom habitats in Inútil Bay, Strait of Magellan, during the austral winter. Abundances are expressed in ind. m⁻². Median, 25th percentile (25Q), and 75th percentile (75Q) values are provided for each taxon, along with its percentage of relative dominance (%) within the assemblage.

Phylum	Class	Order	Family	Taxa	Median	25Q	75Q	%
Annelida	Polychaeta	Terebellida	Ampharetidae	<i>Amage</i> sp.	13.4	13.4	13.4	0.066
Annelida	Polychaeta	Terebellida	Ampharetidae	<i>Ampharete</i> sp.	10.05	6.7	13.4	0.098
Annelida	Polychaeta	Terebellida	Ampharetidae	<i>Anobothrus</i> sp.	13.4	13.4	13.4	0.066
Annelida	Polychaeta	Terebellida	Ampharetidae	<i>Phyllocomus</i> sp.	26.8	26.8	26.8	0.131
Annelida	Polychaeta	Amphinomida	Amphinomidae	<i>Paramphinome australis</i>	10.05	6.7	13.4	0.098
Annelida	Polychaeta	—	Apistobranchidae	<i>Apistobranchus</i> spp.	1.5	1.5	1.5	0.007
Annelida	Polychaeta	Capitellida	Capitellidae	<i>Capitella</i> spp.	204.35	76.275	400.325	8.993
Annelida	Polychaeta	Capitellida	Capitellidae	<i>Notomastus</i> sp.	6.7	6.7	6.7	0.033
Annelida	Polychaeta	Canalipalpata	Chaetopteridae	<i>Chaetopterus variopedatus</i>	13.4	6.7	16.75	0.180
Annelida	Polychaeta	Cirratulida	Cirratulidae	<i>Aphelochaeta</i> spp.	13.4	6.7	469	6.617
Annelida	Polychaeta	Cirratulida	Cirratulidae	<i>Cirratulus cirratus</i>	6.7	6.7	6.7	0.066
Annelida	Polychaeta	Cirratulida	Paraonidae	<i>Kirkegaardia</i> spp.	6.7	6.7	46.9	0.557
Annelida	Polychaeta	Cirratulida	Cirratulidae	<i>Tharyx</i> spp.	244.55	22.45	529.3	13.477
Annelida	Polychaeta	Cossurida	Cossuridae	<i>Cossura</i> spp.	46.9	13.4	93.8	0.753
Annelida	Polychaeta	Terebellida	Flabelligeridae	<i>Flabelligera</i> sp.	6.7	6.7	6.7	0.033
Annelida	Polychaeta	Phyllodocida	Glyceridae	<i>Glycera</i> sp.	13.4	6.3	24.5	0.495
Annelida	Polychaeta	Eunicida	Onuphidae	<i>Hemipodia</i> sp.	17.85	4.925	92.125	1.568
Annelida	Polychaeta	Phyllodocida	Hesionidae	<i>Psamathe</i> sp.	6.7	2.8	11.725	0.138
Annelida	Polychaeta	Eunicida	Lumbrineridae	<i>Lumbrineris</i> spp.	20.1	2.225	48.575	1.117
Annelida	Polychaeta	Eunicida	Lumbrineridae	<i>Ninoe</i> sp.	13.4	13.4	13.4	0.131
Annelida	Polychaeta	Spionida	Magelonidae	<i>Magelona</i> sp.	6.7	6.7	6.7	0.033
Annelida	Polychaeta	Terebellida	Ampharetidae	<i>Asychis</i> sp.	6.7	1.5	6.7	0.073
Annelida	Polychaeta	Maldanida	Maldanidae	<i>Clymenella minor</i>	4.4	2.1	6.7	0.086
Annelida	Polychaeta	Terebellida	Terebellidae	<i>Nicomache</i> sp.	6.7	6.7	6.7	0.033
Annelida	Polychaeta	Phyllodocida	Hesionidae	<i>Isolda viridis</i>	10.05	4.825	23.45	0.250
Annelida	Polychaeta	Phyllodocida	Nephtyidae	<i>Aglaophamus heteroserrata</i>	134	17.2	174.2	3.715
Annelida	Polychaeta	Phyllodocida	Nephtyidae	<i>Aglaophamus</i> sp.	22	92.125	73.7	1.492
Annelida	Polychaeta	Eunicida	Onuphidae	<i>Eunereis patagonica</i>	3.15	3.15	3.15	0.015
Annelida	Polychaeta	Phyllodocida	Nereididae	<i>Nereididae</i> sp.	6.7	6.7	6.7	0.033
Annelida	Polychaeta	Phyllodocida	Nereididae	<i>Nicon</i> spp.	6.7	6.7	6.7	0.066
Annelida	Polychaeta	Phyllodocida	Nereididae	<i>Perinereis</i> sp.	13.4	6.7	14.45	0.169
Annelida	Polychaeta	Phyllodocida	Nereididae	<i>Platynereis</i> sp.	4.1	1.5	6.7	0.040
Annelida	Polychaeta	Eunicida	Onuphidae	<i>Drilonereis</i> sp.	6.7	6.7	6.7	0.066
Annelida	Polychaeta	Opheliida	Opheliidae	<i>Ophelina</i> sp.	6.7	5.55	6.7	0.153

Table A4. Cont.

Phylum	Class	Order	Family	Taxa	Median	25Q	75Q	%
Annelida	Polychaeta	Phyllodocida	Nereididae	<i>Nainereis</i> sp.	6.7	6.7	6.7	0.033
Annelida	Polychaeta	Orbiniida	Orbiniidae	<i>Orbiniia</i> sp.	6.7	6.7	6.7	0.033
Annelida	Polychaeta	Orbiniida	Orbiniidae	<i>Phylo felix</i>	6.7	6.7	6.7	0.033
Annelida	Polychaeta	Orbiniida	Orbiniidae	<i>Scoloplos</i> spp.	2.1	2.1	2.1	0.010
Annelida	Polychaeta	Spionida	Paraonidae	<i>Aricidea</i> spp.	348.4	58.625	842.525	19.596
Annelida	Polychaeta	Maldanida	Maldanidae	<i>Levinseria</i> sp.	8.8	2.1	26.8	0.184
Annelida	Polychaeta	Terebellida	Pectinariidae	<i>Austrophyllosp</i> sp.	6.7	6.7	6.7	0.033
Annelida	Polychaeta	Phyllodocida	Phyllodocidae	<i>Eteone</i> sp.	6.7	6.7	10.05	0.197
Annelida	Polychaeta	Phyllodocida	Phyllodocidae	<i>Nereiphylla</i> sp.	6.7	6.7	6.7	0.033
Annelida	—	Echiura	—	Echiura	44.6	44.6	44.6	0.218
Sipuncula	—	—	—	Sipuncula	6.7	6.7	13.4	0.369
Annelida	Polychaeta	Phyllodocida	Polynoidae	<i>Harmothoe</i> spp.	7.225	2.1	31.825	0.626
Annelida	Polychaeta	Terebellida	Sabellariidae	<i>Idanthyrsus macropaleus</i>	6.7	4.4	6.7	0.141
Annelida	Polychaeta	Sabellida	Sabellariidae	<i>Phragmatopoma</i> sp.	6.7	6.7	6.7	0.033
Annelida	Polychaeta	Sabellida	Sabellidae	<i>Chone</i> sp.	6.7	3.15	13.4	0.114
Annelida	Polychaeta	Sabellida	Sabellidae	<i>Notaulax phaeotaenia</i>	5.25	2.1	13.4	0.101
Annelida	Polychaeta	Terebellida	Terebellidae	<i>Perkinsiana</i> spp.	13.4	6.7	33.5	0.262
Annelida	Polychaeta	Opheliida	Scalibregmatidae	<i>Scalibregma inflatum</i>	6.7	6.7	6.7	0.098
Annelida	Polychaeta	Sabellida	Serpulidae	<i>Apomatus</i> sp.	6.7	6.7	6.7	0.033
Annelida	Polychaeta	Sabellida	Serpulidae	<i>Helicosiphon</i> sp.	6.7	6.7	6.7	0.033
Annelida	Polychaeta	Sabellida	Serpulidae	<i>Hyalopomatus nigropileatus</i>	4.1	1.5	6.7	0.040
Annelida	Polychaeta	Sabellida	Serpulidae	<i>Serpula narconensis</i>	10.05	3.25	159.125	0.190
Annelida	Polychaeta	Sabellida	Serpulidae	<i>Vermiliopsis</i> sp.	6.7	6.7	6.7	0.033
Annelida	Polychaeta	Phyllodocida	Sigalionidae	<i>Leanira quatrefagesi</i>	8.9	4.4	13.4	0.087
Annelida	Polychaeta	Phyllodocida	Pholoidae	<i>Pholoe</i> sp.	6.7	6.7	6.7	0.033
Annelida	Polychaeta	Spionida	Spionidae	<i>Boccardia</i> sp.	6.7	6.55	21.775	0.228
Annelida	Polychaeta	Spionida	Spionidae	<i>Malacoceros</i> sp.	6.7	6.7	6.7	0.033
Annelida	Polychaeta	Spionida	Spionidae	<i>Polydora</i> sp.	7.125	6.7	7.55	0.070
Annelida	Polychaeta	Spionida	Spionidae	<i>Prionospio</i> spp.	6.7	4.1	40.2	0.466
Annelida	Polychaeta	Spionida	Spionidae	<i>Spiophanes</i> sp.	4.4	1.65	51.925	0.378
Annelida	Polychaeta	Phyllodocida	Syllidae	<i>Exogone</i> spp.	6.7	6.075	544.375	1.052
Annelida	Polychaeta	Phyllodocida	Syllidae	Syllidae	10.05	3.25	242.875	0.493
Annelida	Polychaeta	Terebellida	Terebellidae	<i>Amphitrite</i> sp.	6.7	6.7	6.7	0.033
Annelida	Polychaeta	Terebellida	Terebellidae	<i>Artacama</i> sp.	4.4	4.4	4.4	0.022
Annelida	Polychaeta	Terebellida	Terebellidae	<i>Leaena</i> spp.	6.7	2.1	6.7	0.076
Annelida	Polychaeta	Terebellida	Terebellidae	<i>Streblosoma</i> sp.	10.05	6.7	13.4	0.098
Annelida	Polychaeta	Terebellida	Terebellidae	<i>Terebella</i> sp.	6.7	6.7	6.7	0.033
Annelida	Polychaeta	Terebellida	Terebellidae	<i>Thelepus</i> spp.	6.7	6.7	7.75	0.103
Annelida	Polychaeta	Opheliida	Opheliidae	<i>Travisia</i> sp.	10.05	2.8	28.475	0.269
Annelida	Polychaeta	Terebellida	Trichobranchidae	<i>Terebellides stroemi</i>	6.7	6.7	6.7	0.033
Annelida	Polychaeta	Terebellida	Trichobranchidae	<i>Trichobranchus</i> spp.	6.3	6.3	6.3	0.031
Priapulida	—	—	—	Priapulida	6.3	6.3	6.3	0.031
Arthropoda	Pycnogonida	—	—	Pycnogonida	6.7	6.7	13.4	0.131
Arthropoda	Copepoda	—	—	Copepoda	6.7	6.7	6.7	0.033
Arthropoda	Ostracoda	—	—	Ostracoda	8.4	6.7	13.4	0.139
Arthropoda	Malacostraca	Decapoda	Paguridae	<i>Pagurus</i> sp.	6.7	6.7	6.7	0.033
Arthropoda	Malacostraca	Decapoda	Pinnotheridae	<i>Pinnixa</i> sp.	4.4	2.1	6.7	0.043
Arthropoda	Malacostraca	Amphipoda	Aoridae	<i>Aora</i> sp.	7.75	2.1	13.4	0.076
Arthropoda	Malacostraca	Amphipoda	Caprellidae	Caprellidae	6.7	6.7	6.7	0.033
Arthropoda	Malacostraca	Amphipoda	Phoxocephalidae	<i>Cephalophoxoides</i> sp.	6.7	1.5	73.7	0.400
Arthropoda	Malacostraca	Amphipoda	—	Cheirocratidae	2.1	2.1	13.4	0.162
Arthropoda	Copepoda	Harpacticoida	Cletodidae	<i>Cletodes</i> sp.	10.05	6.7	13.4	0.197
Arthropoda	Malacostraca	Cumacea	—	Cumacea	13.4	3.15	30.15	0.391
Arthropoda	Malacostraca	Cumacea	Diastylidae	Diastylidae	6.7	6.7	6.7	0.033
Arthropoda	Malacostraca	Amphipoda	Phoxocephalidae	<i>Fuegiphoxus</i> sp.	53.6	53.6	53.6	0.262
Arthropoda	Malacostraca	Amphipoda	Phoxocephalidae	<i>Fuegiphoxus uncinatus</i>	6.7	6.7	6.7	0.066
Arthropoda	Malacostraca	Isopoda	—	Isopoda	13.4	13.4	13.4	0.066
Arthropoda	Malacostraca	Amphipoda	Lysianassoidea	Lysianassoidea	6.7	6.7	6.7	0.033
Arthropoda	Malacostraca	Amphipoda	Corophiidae	<i>Monocorophium</i> sp.	6.7	6.7	13.4	1.845

Table A4. Cont.

Phylum	Class	Order	Family	Taxa	Median	25Q	75Q	%
Arthropoda	Malacostraca	Amphipoda	Oedicerotidae	Oedicerotidae	5.55	4.4	6.7	0.054
Arthropoda	Malacostraca	Amphipoda	Phoxocephalidae	Phoxocephalidae	10.575	6.7	14.45	0.103
Arthropoda	Malacostraca	Amphipoda	Phoxocephalidae	Phoxocephalinae	6.7	6.7	6.7	0.033
Arthropoda	Malacostraca	Amphipoda	—	<i>Pseudiphimediella glabra</i>	6.7	6.7	6.7	0.033
Arthropoda	Malacostraca	Amphipoda	Stenothoidae	Stenothoidae	7.75	6.7	37.375	0.338
Arthropoda	Malacostraca	Tanaidacea	—	Tanaidacea	7.55	34.625	23.45	0.481
Arthropoda	Malacostraca	Amphipoda	Uristidae	<i>Uristes schellenbergi</i>	6.7	6.7	6.7	0.066
Arthropoda	Malacostraca	Amphipoda	Urothoidae	<i>Urothoe falcata</i>	6.7	6.7	33.5	0.229
Arthropoda	Malacostraca	Amphipoda	Urothoidae	Urothoidae	6.7	6.7	6.7	0.033
Arthropoda	Hexanauplia	Thecostraca	—	Cirripedia	2.1	2.1	2.1	0.010
Brachiopoda	Rhynchonellata	Terebratulida	Terebratellidae	<i>Magellania venosa</i>	77.05	3.525	244.55	4.122
Cnidaria	Anthozoa	Actiniaria	Edwardsiidae	<i>Edwardsia</i> sp.	6.7	6.7	6.7	0.033
Echinodermata	Asteroidea	—	—	Asteroidea	1.5	1.5	1.5	0.007
Echinodermata	Echinoidea	—	—	Echinoidea	6.7	2.1	13.4	0.109
Echinodermata	Holothuroidea	Dendrochirotida	Psolidae	<i>Psolus</i> sp.	13.4	6.7	13.4	0.262
Echinodermata	Ophiuroidea	—	—	Ophiuroidea	26.8	26.8	26.8	0.131
Entoprocta	—	—	Pedicellinidae	<i>Pedicellina cernua</i>	13.4	13.4	13.4	0.066
Mollusca	Bivalvia	Cardiida	Carditidae	<i>Cyclocardia thouarsii</i>	14.675	8.175	242.875	0.307
Mollusca	Bivalvia	Venerida	Veneridae	<i>Eurhomalea</i> sp.	26.8	26.8	26.8	0.131
Mollusca	Bivalvia	Adapedonta	Hiatellidae	<i>Hiatella</i> sp.	27.85	27.85	27.85	0.136
Mollusca	Bivalvia	Mytilida	Mytilidae	Mytilidae	7.75	2.1	13.4	0.076
Mollusca	Bivalvia	Nuculida	Nuculidae	<i>Nucula</i> spp.	6.7	5.25	13.4	0.303
Mollusca	Bivalvia	Nuculanida	Neilonellidae	<i>Pseudoneilonella</i> sp.	26.8	13.4	110.55	1.343
Mollusca	Bivalvia	Lucinida	Thyasiridae	<i>Thyasira</i> sp.	26.8	12.8	368.5	3.859
Mollusca	Bivalvia	Nuculanida	Yoldiidae	<i>Yoldiella</i> sp.	30.15	4.975	139.025	1.135
Mollusca	Bivalvia	Pectinida	Pectinidae	<i>Zygochlamys patagonica</i>	6.7	4.4	20.1	0.272
Mollusca	Gastropoda	Acteonida	Acteonidae	<i>Acteon</i> sp.	7.75	2.1	13.4	0.114
Mollusca	Gastropoda	Littorinimorpha	Calyptaeidae	Calyptaeidae	5.55	4.4	6.7	0.054
Mollusca	Gastropoda	Caenogastropoda	Cerithiidae	<i>Cerithidium</i> sp.	8.4	6.7	20.1	0.303
Mollusca	Gastropoda	Caenogastropoda	—	<i>Colpospirella</i> sp.	29.95	6.7	33.5	0.343
Mollusca	Gastropoda	Littorinimorpha	Cymatiidae	<i>Fusitriton</i> sp.	10.05	6.7	13.4	0.033
Mollusca	Gastropoda	Vetigastropoda	Lepetidae	<i>Iothia</i> sp.	10.05	5.55	41.375	0.782
Mollusca	Gastropoda	Nudibranchia	—	Nudibranchia	6.7	6.7	6.7	0.033
Mollusca	Gastropoda	Neogastropoda	Cominellidae	<i>Pareuthria</i> sp. 1	10.05	6.7	23.45	0.262
Mollusca	Gastropoda	Neogastropoda	Cominellidae	<i>Pareuthria</i> sp. 2	45.225	108.875	87.1	0.934
Mollusca	Polyplacophora	Chitonida	Callochitonidae	<i>Callochiton</i> sp.	6.7	6.7	6.7	0.066
Mollusca	Polyplacophora	Chitonida	Chitonidae	<i>Chiton</i> sp.	13.4	13.4	13.4	0.066
Mollusca	Polyplacophora	Chitonida	Ischnochitonidae	<i>Lepidozona</i> sp.	13.4	13.4	13.4	0.066
Mollusca	Polyplacophora	Lepidopleurida	Lepidopleuridae	<i>Leptochiton</i> sp.	2.1	1.5	38.95	0.406
Mollusca	Polyplacophora	Chitonida	Chitonidae	<i>Tonicia</i> sp.	13.4	13.4	13.4	0.066
Nematoda	—	—	—	Nematoda	50.25	26.8	335	10.361
Nemertea	—	—	—	Nemertea	27.85	2.1	53.6	0.272
Phoronida	—	—	Phoronidae	<i>Phoronis</i> sp.	154.1	154.1	154.1	0.753

References

- Food and Agriculture Organization of the United Nations (FAO). Global Forest Resources Assessment 2000. Chapter 5: Forest Management and Conservation. In *FAO Forestry Paper No. 140*; FAO: Rome, Italy, 2001; 479p.
- Ballesteros, M.; Hopkins, A.; Salicrú, M.; Nimbs, M.J. Heterobranch Sea Slugs s.l. (Mollusca, Gastropoda) from the Southern Ocean: Biodiversity and Taxonomy. *Diversity* **2025**, *17*, 330. [\[CrossRef\]](#)
- Quiñones, R.A.; Fuentes, M.; Montes, R.M.; Soto, D.; León-Muñoz, J. Environmental issues in Chilean salmon farming: A review. *Rev. Aquac.* **2019**, *11*, 375–402. [\[CrossRef\]](#)
- Buschmann, A.H.; Niklitschek, E.J.; Pereda, S.V. Aquaculture and Its Impacts on the Conservation of Chilean Patagonia. In *Conservation in Chilean Patagonia*; Castilla, J.C., Armesto Zamudio, J.J., Martínez-Harms, M.J., Tecklin, D., Eds.; Integrated Science; Springer: Cham, Switzerland, 2023; Volume 19, pp. 303–320. [\[CrossRef\]](#)
- Norambuena, H.V.; Labra, F.A.; Matus, R.; Gómez, H.; Luna-Quevedo, D.; Espoz, C. Green energy threatens Chile's Magallanes Region. *Science* **2022**, *376*, 361–362. [\[CrossRef\]](#)

6. Acosta, K.; Salazar, I.; Saldaña, M.; Ramos, J.; Navarra, A.; Toro, N. Chile and Its Potential Role among the Most Affordable Green Hydrogen Producers in the World. *Front. Environ. Sci.* **2022**, *10*, 890104. [[CrossRef](#)]
7. Molinet, C.; Niklitschek, E.J. Fisheries and Marine Conservation in Chilean Patagonia. In *Conservation in Chilean Patagonia*; Castilla, J.C., Armesto Zamudio, J.J., Martínez-Harms, M.J., Tecklin, D., Eds.; Integrated Science; Springer: Cham, Switzerland, 2023; Volume 19, pp. 283–301. [[CrossRef](#)]
8. Palma, S. Zooplankton distribution and abundance in the austral Chilean channels and fjords. In *Progress in the Oceanographic Knowledge of Chilean Interior Waters, from Puerto Montt to Cape Horn*; Silva, N., Palma, S., Eds.; Comité Oceanográfico Nacional–Pontificia Universidad Católica de Valparaíso: Valparaíso, Chile, 2008; pp. 107–113.
9. Bernal, R.; Balbontín, F. Distribución y abundancia de las larvas de peces desde el estrecho de Magallanes al cabo de Hornos. *Rev. Cienc. Tecnol. Mar* **2003**, *26*, 85–92.
10. Salas-Berrios, F.; Valdés-Aguilera, J.; Landaeta, M.F.; Bustos, C.A.; Pérez-Vargas, A.; Balbontín, F. Feeding habits and diet overlap of marine fish larvae from the peri-Antarctic Magellan region. *Polar Biol.* **2013**, *36*, 1401–1414. [[CrossRef](#)]
11. Zagami, G.; Antezana, T.; Ferrari, I.; Granata, A.; Sitran, R.; Minutoli, R.; Guglielmo, L. Species diversity, spatial distribution, and assemblages of zooplankton within the Strait of Magellan in austral summer. *Polar Biol.* **2011**, *34*, 1319–1333. [[CrossRef](#)]
12. Palma, S.; Aravena, G. Distribución de Quetognatos, Eufáusidos y Sifonóforos en la región Magallánica. *Rev. Cienc. Tecnol. Mar* **2001**, *24*, 47–59.
13. Cañete, J.I.; Gallardo, C.S.; Olave, C.; Romero, M.S.; Figueroa, T.; Haro, D. Abundance and spatial distribution of neustonic copepodids of *Microsetella rosea* (Harpacticoida: Ectinosomatidae) along the western Magellan coast, southern Chile. *Lat. Am. J. Aquat. Res.* **2016**, *44*, 576–587. [[CrossRef](#)]
14. Gambi, M.C.; Giangrande, A. Polychaetes of the soft bottoms of the Straits of Magellan collected during the Italian oceanographic cruise in February–March 1991. *An. Inst. Patagon.* **1993**, *21*, 179–192.
15. Thatje, S.; Brown, A. The macrobenthic ecology of the Straits of Magellan and the Beagle Channel. *An. Inst. Patagon.* **2009**, *37*, 17–27. [[CrossRef](#)]
16. Jara, N.; Montiel, A.; Céceres, B. The Roles of Alpha, Beta, and Functional Diversity Indices in the Ecological Connectivity between Two Sub-Antarctic Macrofaunal Assemblages. *Diversity* **2024**, *16*, 430. [[CrossRef](#)]
17. Mutschke, E.; Ríos, C. Distribución espacial y abundancia relativa de equinodermos en el Estrecho de Magallanes, Chile. *Rev. Cienc. Tecnol. Mar* **2006**, *29*, 91–102.
18. Ríos, C.; Mutschke, E.; Montiel, A.; Gerdes, D.; Arntz, W.E. Soft-bottom macrobenthic faunal associations in the southern Chilean glacial fjord complex. *Sci. Mar.* **2005**, *69* (Suppl. 2), 225–236. [[CrossRef](#)]
19. Ríos, C.; Mutschke, E. Community structure of intertidal boulder-cobble fields in the Strait of Magellan, Chile. *Sci. Mar.* **1999**, *63* (Suppl. 1), 193–201. [[CrossRef](#)]
20. Lange, I.D.; Perry, C.T. A quick, easy and non-invasive method to quantify coral growth rates using photogrammetry and 3D model comparisons. *Methods Ecol. Evol.* **2020**, *11*, 714–726. [[CrossRef](#)]
21. Bicknell, A.W.; Godley, B.J.; Sheehan, E.V.; Votier, S.C.; Witt, M.J. Camera technology for monitoring marine biodiversity and human impact. *Front. Ecol. Environ.* **2016**, *14*, 424–432. [[CrossRef](#)]
22. Gutt, J.; Helsen, E.; Arntz, W.; Buschmann, A. Biodiversity and community structure of the mega-epibenthos in the Magellan region (South America). *Sci. Mar.* **1999**, *63* (Suppl. S1), 155–170. [[CrossRef](#)]
23. Friedlander, A.M.; Ballesteros, E.; Caselle, J.E.; Hüne, M.; Adler, A.M.; Sala, E. Patterns and drivers of benthic macroinvertebrate assemblages in the kelp forests of southern Patagonia. *PLoS ONE* **2023**, *18*, e0279200. [[CrossRef](#)]
24. Cárdenas, C.; Montiel, A. The influence of depth and substrate inclination on sessile assemblages in subantarctic rocky reefs (Magellan region). *Polar Biol.* **2015**, *38*, 1631–1644. [[CrossRef](#)]
25. Villalobos, V.; Valdivia, N.; Försterra, G.; Ballyman, S.; Espinoza, J.; Wadham, J.; Burgos-Andrade, K.; Häussermann, V. Depth-dependent diversity patterns of rocky subtidal macrobenthic communities along a temperate fjord in Northern Chilean Patagonia. *Front. Mar. Sci.* **2021**, *8*, 635855. [[CrossRef](#)]
26. Betti, F.; Bavestrello, G.; Bo, M.; Enrichetti, F.; Loi, A.; Wanderlingh, A.; Pérez-Santos, I.; Daneri, G. Benthic biodiversity and ecological gradients in the Seno Magdalena (Puyuhuapi Fjord, Chile). *Estuar. Coast. Shelf Sci.* **2017**, *198*, 269–278. [[CrossRef](#)]
27. Ortiz, P.; Hamamé, M. Distribución de las comunidades epibentónicas y caracterización de hábitats en el fiordo Puyuhuapi, Patagonia Norte. *An. Inst. Patagon.* **2022**, *50*, 1–19. [[CrossRef](#)]
28. Zapata, G.; Gorny, M.; Montiel, A. Filling ecological gaps in Chilean Central Patagonia: Patterns of biodiversity and distribution of sublittoral benthic invertebrates from the Katalalixar National Reserve waters (~48°S). *Front. Mar. Sci.* **2022**, *9*, 951195. [[CrossRef](#)]
29. Rovira, J.; Herreros, J. *Clasificación de Ecosistemas Marinos Chilenos de la Zona Económica Exclusiva*; Ministerio del Medio Ambiente: Santiago, Chile, 2016.
30. Spalding, M.D.; Fox, H.E.; Allen, G.R.; Davidson, N.; Ferdaña, Z.A.; Finlayson, M.; Halpern, B.S.; Jorge, M.A.; Lombana, A.; Lourie, S.A.; et al. Marine ecoregions of the world: A bioregionalization of coastal and shelf areas. *Bioscience* **2007**, *57*, 573–583. [[CrossRef](#)]

31. Panella, S.; Michelato, A.; Perdicaro, R.; Magazzú, G.; Decembrini, F.; Scarazzato, P. A preliminary contribution to understanding the hydrological characteristics of the Strait of Magellan: Austral spring 1989. *Boll. Oceanol. Teor. Appl.* **1991**, *9*, 107–126.

32. Brambati, A. Introduction to the Magellan Project. *Boll. Oceanol. Teor. Appl.* **1991**, *9*, 83–92.

33. Valdenegro Mancilla, A. Caracterización Oceanográfica Física y Química de la Zona de Canales y Fiordos Australes de Chile Entre el Estrecho de Magallanes y Cabo de Hornos (Cimar 3 Fiordo). Bachelor’s Thesis, Escuela de Ciencias del Mar, Facultad de Recursos Naturales, Universidad Católica de Valparaíso, Valparaíso, Chile, 2002.

34. Boltovskoy, D. *Atlas del Zooplancton del Atlántico Sudoccidental y Métodos de Trabajo con el Zooplancton Marino*; INIDEP: Mar del Plata, Argentina, 1981.

35. Guglielmo, L.; Ianora, A. Atlas of Marine Zooplankton: Straits of Magellan. In *Amphipods, Euphausiids, Mysids, Ostracods, and Chaetognaths*; Springer: Berlin/Heidelberg, Germany, 1997. [\[CrossRef\]](#)

36. Guglielmo, L.; Ianora, A. (Eds.) *Atlas of Marine Zooplankton: Straits of Magellan. Copepods*; Springer: Berlin/Heidelberg, Germany; New York, NY, USA, 1995; 279p.

37. Smith, D.B.L.; Johnson, K.B. *A Guide to Marine Coastal Plankton and Marine Invertebrate Larvae*, 2nd ed.; Kendall/Hunt Publishing Company: Dubuque, IA, USA, 1996.

38. Tagliapietra, D.; Sigovini, M. Benthic fauna: Collection and identification of macrobenthic invertebrates. *Terre Environ.* **2010**, *88*, 253–261.

39. Ontrup, J.; Ehnert, N.; Bergmann, M.; Nattkemper, T.W. BIIGLE—Web 2.0 enabled labelling and exploring of images from the Arctic deep sea observatory HAUSGARTEN. In Proceedings of the OCEANS 2009–Europe, Bremen, Germany, 11–14 May 2009; IEEE: Piscataway, NJ, USA, 2009; pp. 1–7. [\[CrossRef\]](#)

40. Castellanos, Z.J.A. Catálogo descriptivo de la malacofauna magallánica 8. In *Neogastropoda, Columbellidae, Pyrenidae, Cominellidae y Fascioliidae*; Comisión de Investigaciones Científicas, Provincia de Buenos Aires: Buenos Aires, Argentina, 1992; 41p.

41. Hartman, O. Polychaeta Errantia of Antarctica. *Antarct. Res. Ser.* **1964**, *3*, 1–131.

42. Hartman, O. Polychaeta Myzostomidae and Sedentaria of Antarctica. *Antarct. Res. Ser.* **1966**, *7*, 1–158.

43. Licher, F. Revision der Gattung *Typosyllis* Langerhans, 1879 (Polychaeta: Syllidae) Morphologie, taxonomie und phylogenie. *Abh. Senckenberg. Naturforschenden Ges.* **1999**, *551*, 1–363.

44. Böggemann, M. Revision of the Glyceridae Grube 1850 (Annelida: Polychaeta). *Abh. Senckenberg. Naturforschenden Ges.* **2002**, *555*, 1–249.

45. Wilson, R.S.; Hutchings, P.A.; Glasby, C.J. *Polychaetes: An Interactive Identification Guide*; CSIRO Publishing: Melbourne, Australia, 2003.

46. Häussermann, V.; Försterra, G. *Fauna Marina Bentónica de la Patagonia Chilena. Guía de Identificación Ilustrada*; Nature in Focus: Santiago, Chile, 2009; 1000p, ISBN 978-956-332-244-6.

47. Hammer, Ø.; Harper, D.A.T.; Ryan, P.D. PAST: Paleontological statistics software package for education and data analysis. *Palaeontol. Electron.* **2001**, *4*, 1–9.

48. Jones, F.C. Taxonomic sufficiency: The influence of taxonomic resolution on freshwater bioassessments using benthic macroinvertebrates. *Environ. Rev.* **2008**, *16*, 45–69. [\[CrossRef\]](#)

49. Clarke, K.R.; Gorley, R.N. *PRIMER v7: User Manual/Tutorial*; PRIMER-E: Plymouth, UK, 2015.

50. Brasier, M.J.; Barnes, D.K.A.; Bax, N.; Brandt, A.; Christianson, A.B.; Constable, A.J.; Downey, R.; Figuerola, B.; Griffiths, H.; Gutt, J.; et al. Responses of Southern Ocean seafloor habitats and communities to global and local drivers of change. *Front. Mar. Sci.* **2021**, *8*, 622721. [\[CrossRef\]](#)

51. Landaeta, M.F.; Skamiotis, K.; Lara, P.; Olivera, F. Spatio-temporal variations in the mesozooplankton assemblages off Clarence Island, Magellan Strait, Chile. *Reg. Stud. Mar. Sci.* **2024**, *73*, 103507. [\[CrossRef\]](#)

52. Balbontín, F.; Bernal, R. Cambios estacionales en la composición y abundancia del ictioplankton de los canales australes entre el Golfo Corcovado y Golfo Elefantes, Chile. *Rev. Cienc. Tecnol. Mar.* **2005**, *28*, 99–111.

53. Biancalana, F.; Dutto, M.S.; Berasategui, A.A.; Kopprio, G.; Hoffmeyer, M.S. Mesozooplankton assemblages and their relationship with environmental variables: A study case in a disturbed bay (Beagle Channel, Argentina). *Environ. Monit. Assess.* **2014**, *186*, 8629–8647. [\[CrossRef\]](#)

54. Suárez-Morales, E.; Gasca, R. *Cymbasoma bowmani* sp. nov., a new monstrilloid (Copepoda: Monstrilloida) from a Caribbean reef, with notes on species variation. *J. Mar. Syst.* **1998**, *15*, 433–439. [\[CrossRef\]](#)

55. Suárez-Morales, E.; Castellanos-Osorio, I.A. A new species of Monstrilla (Copepoda, Monstrilloida) from the plankton of a large coastal system of the northwestern Caribbean with a key to species. *ZooKeys* **2019**, *876*, 111–123. [\[CrossRef\]](#)

56. Angel, M.V.; Blachowiak-Samolyk, K. Halocyprid ostracods of the Southern Ocean. In *Biogeographic Atlas of the Southern Ocean*; De Broyer, C., Koubbi, P., Griffiths, H.J., Raymond, B., Udekem d’Acoz, C.d’, Eds.; Scientific Committee on Antarctic Research: Cambridge, UK, 2014; pp. 297–302.

57. Hamamé, M.; Antezana, T. Chlorophyll and zooplankton in microbasins along the Straits of Magellan–Beagle Channel passage. *Sci. Mar.* **1999**, *63* (Suppl. 1), 35–42. [\[CrossRef\]](#)

58. Gorny, M.; Pereda, R. Descripción de la composición y distribución geográfica de ictiofauna bentónica por medio de imágenes submarinas en las aguas interiores de la Reserva Nacional Katalalixar (Patagonia Central Chilena). *An. Inst. Patagon.* **2022**, *50*, 1–14. [[CrossRef](#)]

59. Gorny, M.M. Proyecto D001I1181. In *Desarrollo de la Pesquería de Langostino de los Canales (Munida subrugosa) en la XII Región, Magallanes y Antártica Chilena*; Universidad de Magallanes: Punta Arenas, Chile, 2000; Proyecto FONDEF, Octavo Concurso Nacional de Proyectos de I+D.

60. Thatje, S.; Schnack-Schiel, S.; Arntz, W.E. Developmental trade-offs in Subantarctic meroplankton communities and the enigma of low decapod diversity in high southern latitudes. *Mar. Ecol. Prog. Ser.* **2003**, *260*, 195–207. [[CrossRef](#)]

61. Sabatini, M.E.; Giménez, J.; Rocco, V. Características del zooplancton del área costera de la plataforma patagónica austral (Argentina). *Bol. Inst. Español Oceanogr.* **2001**, *17*, 245–254. Available online: <http://hdl.handle.net/11336/41896> (accessed on 13 July 2025).

62. Bowden, D.A.; Clarke, A.; Peck, L.S. Seasonal variation in the diversity and abundance of pelagic larvae of Antarctic marine invertebrates. *Mar. Biol.* **2009**, *156*, 2033–2047. [[CrossRef](#)]

63. Nahuelhual, L.; Saavedra, G.; Mellado, M.A.; Vergara, X.; Vallejos, T. A social-ecological trap perspective to explain the emergence and persistence of illegal fishing in small-scale fisheries. *Marit. Stud.* **2020**, *19*, 105–117. [[CrossRef](#)]

64. Zimmerling, J.R.; Pomeroy, A.C.; d'Entremont, M.V.; Francis, C.M. Canadian estimate of bird mortality due to collisions and direct habitat loss associated with wind turbine developments. *Avian Conserv. Ecol.* **2013**, *8*, 10. [[CrossRef](#)]

65. Solé, M.; Kaifu, K.; Mooney, T.A.; Nedelec, S.L.; Olivier, F.; Radford, A.N.; Vazzana, M.; Wale, M.A.; Semmens, J.M.; Simpson, S.D.; et al. Effects of anthropogenic noise on marine invertebrates. *Front. Mar. Sci.* **2023**, *10*, 1129057. [[CrossRef](#)]

66. Green, R.; Higginbottom, K. *The Negative Effects of Wildlife Tourism on Wildlife (Wildlife Tourism Report Series No. 5)*; CRC for Sustainable Tourism Pty Ltd.: Gold Coast, Australia, 2001. [[CrossRef](#)]

67. Sanderson, E.W.; Redford, K.H.; Chetkiewicz, C.-L.B.; Medellín, R.R.; Rabinowitz, A.R.; Robinson, J.G.; Taber, A.B. Planning to save a species: The jaguar as a model. *Conserv. Biol.* **2002**, *16*, 58–72. [[CrossRef](#)]

68. Noss, R.F. Landscape connectivity: Different functions at different scales. In *Landscape Linkage and Biodiversity*; Hudson, W.E., Ed.; Island Press: Washington, DC, USA, 1991; pp. 27–39.

69. García Quiroga, F. La problemática de la expansión geográfica de las especies exóticas invasoras. Análisis y distribución de dos especies en la provincia de Ávila e iniciativas para la minimización de sus efectos. *Obs. Medioambient.* **2012**, *15*, 175–196. [[CrossRef](#)]

70. Estay, M.; Chávez, C. Location decisions and regulatory changes: The case of the Chilean aquaculture. *Lat. Am. J. Aquat. Res.* **2015**, *43*, 700–717. [[CrossRef](#)]

Disclaimer/Publisher's Note: The statements, opinions and data contained in all publications are solely those of the individual author(s) and contributor(s) and not of MDPI and/or the editor(s). MDPI and/or the editor(s) disclaim responsibility for any injury to people or property resulting from any ideas, methods, instructions or products referred to in the content.